# Genomic Analysis of 220 CTCLs Identifies a Novel Recurrent Gain-of-function Alteration in RLTPR (p.Q575E)

Joonhee Park, Jingyi Yang, Alexander T. Wenzel, Akshaya Ramachandran, Wung J. Lee, Jay C. Daniels, Estela Martinez-Escala, Nduka Amankulor, Barbara Pro, Joan Guitart, Marc L. Mendillo, Jeffrey N. Savas, Titus J. Boggon, and Jaehyuk Choi

23 Supplementary Tables
14 Supplementary Figures

Table of Contents

**Supplemental Table S1. Description of excluded samples from original studies.**

| Study | # of samples in original paper | # of samples included | Excluded samples |
|---|---|---|---|
| Choi et al [1] | 40 | 40 | - |
| Ungewickell et al [2] | 11 | 11 | - |
| McGirt et al [3] | 5 | 5 | - |
| Vaque et al [4] | 11 | 10 | case 11* |
| Kiel et al [5] | 66 | 55 | H01, D02, G01, SS1, SS12, SS19, SS44, SS54, SS58, SS59, SS75** |
| Wang et al [6] | 37 | 37 | - |
| Almeida et al [7] | 42 | 40 | SS_L15, SS_L9*** |
| Woollard et al [8] | 10 | 10 | - |
| Prasad et al [9] | 12 † | 12 | - |

† 12 samples which were available in supplementary table were used in analysis.
* 1 sample without mutation in original paper is excluded
** 11 samples were excluded because they had over 5 single nucleotide variants shared with other samples in their or other datasets raising the possibility they are derived from the same patient.
*** After submitting the mutations through our pipeline, two samples had no mutations remaining.

**Supplemental Table S2. Description of CTCL genetic studies used in analysis.**

| Study | # of samples | Patient characterization | Sequencing type | Somatic mutation | Reports of synonymous mutations |
|---|---|---|---|---|---|
| Choi et al [1] | 40 | SS | Whole exome | yes | yes |
| Ungewickell et al [2] | 11 | MF and SS | Whole exome | yes | no |
| McGirt et al [3] | 5 | MF | Whole genome | yes | yes |
| Vaque et al [4] | 10 | MF and SS | Targeted | yes | no |
| Kiel et al [5] | 55 | SS | Whole exome | no | no |
| Wang et al [6] | 37 | SS | Whole exome | yes | yes |
| Almeida et al [7] | 40 | SS, MF and other CTCL | Whole exome | yes | no |
| Woollard et al [8] | 10 | SS | Whole exome | yes | no |
| Prasad et al [9] | 12 | SS | Whole exome | yes | yes |

MF, Mycosis fungoides; SS, Sezary syndrome; CTCL, cutaneous T cell lymphoma

**Supplemental Table S3. Summary of the primers sequences.**

| Primer | Sequence |
|---|---|
| *RLTPR* cloning Forward | GAAGATTCTAGAGCTAGCGAATTCACCATGGC CCAGACCCCCGAC |
| *RLTPR* cloning Reverse | TCGCAGATCCTTGCGGCCGCGGATCCTCAGG GATTGGGGCCGCCG |
| RLTPR p.Q575E mutagenesis Forward | TGCACCGGATTGTCGAGCTCATGCAGGAC |
| RLTPR p.Q575E mutagenesis Reverse | GTCCTGCATGAGCTCGACAATCCGGTGCA |
| *RLTPR* qPCR Forward | CTGGAGCGGGGAGAAACA |
| *RLTPR* qPCR Reverse | CATCTGAGCCAGCTTTCTTG |
| *IL-2* qPCR Forward | CAAACCTCTGGAGGAAGTGC |
| *IL-2* qPCR Reverse | GGTTGCTGTCTCATCAGCAT |
| *GAPDH* qPCR Forward | GAAGGTGAAGGTCGGAGTC |
| *GAPDH* qPCR Reverse | GAAGATGGTGATGGGATTTC |
| *ARHGEF3* cloning Forward | GAAGATTCTAGAGCTAGCGAATTCACCATGGT GGCCAAGGATTAC |
| *ARHGEF3* cloning Reverse | GCAGATCCTTGCGGCCGCGGATCCTCAGACG TTACTTTCACCGTG |
| ARHGEF3 p.R84H mutagenesis Forward | GAGGATGTCAGGGTGGCTCTCACTGCG |
| ARHGEF3 p.R84H mutagenesis Reverse | CGCAGTGAGAGCCACCCTGACATCCTC |
| ARHGEF3 p.L269E mutagenesis Forward | TGCCTCAAGATTTCTCGGAGCTCCAGAGGGTA TTTTACCAGGC |
| ARHGEF3 p.L269E mutagenesis Reverse | GCCTGGTAAAATACCCTCTGGAGCTCCGAGAA ATCTTGAGGCA |
| *CSNK1A1* cloning Forward | GAAGATTCTAGAGCTAGCGAATTCACCATGGC GAGTAGCAGCGGC |
| *CSNK1A1* cloning Reverse | CGCAGATCCTTGCGGCCGCGGATCCTTAGAAA CCTTTCATGTTAC |
| CK1α p.S27C Forward | GATGTCCCCGAAGCAGCCAGACCCGAT |
| CK1α p.S27C Reverse | ATCGGGTCTGGCTGCTTCGGGGACATC |
| CK1α p.S27F Forward | AGATGTCCCCGAAGAAGCCAGACCCGATC |
| CK1α p.S27F Reverse | GATCGGGTCTGGCTTCTTCGGGGACATCT |
| *CSNK1A1* qPCR Forward | ATGGCGAGTAGCAGCGGCTC |
| *CSNK1A1* qPCR Reverse | CGTATGTGGGGGATGCCAAC |
| RLTPR p.Q575E gDNA sanger sequencing | GGTGATACAAGACTTAGTGTG |

| | | |
|---|---|---|
| | Forward | |
| RLTPR p.Q575E gDNA sanger sequencing | Reverse | GTTGTTCCTCAAGAGACAGG |
| *RLTPR* Exon 14 Forward | | GTTGACACCGCGAGGAAT |
| *RLTPR* Exon 14 Reverse | | TGAGGTCCAGGTGCAGGT |
| *RLTPR* Exon 36 Forward | | GTGTCTGCTGACCCTTCCTG |
| *RLTPR* Exon 36 Reverse | | AGATCCTAGGCTTGGGGATG |

**Supplemental Table S4. Study description according to patient CTCL subtype characterization.**

| Study | Patient characterization | # of samples | # of SS | # of MF | # of CTCL-NOS |
|---|---|---|---|---|---|
| Choi et al | SS | 40 | 40 | 0 | 0 |
| Kiel et al | SS | 55 | 55 | 0 | 0 |
| Wang et al | SS | 37 | 37 | 0 | 0 |
| Woollard et al | SS | 10 | 10 | 0 | 0 |
| Prasad et al | SS | 12 | 12 | 0 | 0 |
| Ungewickell et al | MF and SS | 11 | 5 | 6 | 0 |
| Vaque et al | MF and SS | 10 | 4 | 6 | 0 |
| Almeida et al | SS, MF and CTCL-NOS | 40 | 23 | 8 | 9 |
| McGirt et al | MF | 5 | 0 | 5 | 0 |

**Supplemental Table S5. Genes with a statistically significant burden of gene mutations as assessed by MutSig CV**

| Gene | # of nonsynonymous mutations | # of synonymous mutations | *P* value | Adjusted *P* value* |
|---|---|---|---|---|
| *TP53* | 22 | 0 | 0 | 0 |
| *FAS* | 6 | 0 | 2.39E-06 | 2.26E-02 |
| *CCR4* | 5 | 0 | 5.27E-06 | 3.31E-02 |

* *P* value adjusted for multiple hypothesis testing.

**Supplemental Table S6. Hotspot mutations that occur at the same amino acid more often than expected by chance alone.**

| Gene | Amino acid change | # of total mutations | # of recurrent mutations* | Adjusted *P* value** |
|---|---|---|---|---|
| *PLCG1* | p.S345F | 22 | 8 | 3.38E-24 |
| *RLTPR* | p.Q575E | 7 | 7 | 5.91E-20 |
| *CCR4* | p.Y331X | 7 | 4 | 1.09E-07 |
| *PLCG1* | p.R48W | 22 | 4 | 1.09E-07 |
| *RHOA* | p.N117I; p.N117K | 10 | 4 | 1.09E-07 |
| *PLCG1* | p.E1163K | 22 | 3 | 8.15E-04 |
| *CD28* | p.F51V; p.F51I | 9 | 3 | 8.15E-04 |
| *CARD11* | p.D357N; p.D357E; p.D357A | 13 | 3 | 8.15E-04 |
| *SMARCB1* | p.Q368X | 7 | 3 | 8.15E-04 |
| *CARD11* | p.S615F | 13 | 3 | 8.15E-04 |
| *MAPK1* | p.E322A; p.E322K | 3 | 3 | 8.15E-04 |
| *STAT5B* | p.N642H | 8 | 3 | 8.15E-04 |

Rate of background mutations were determined for each gene and adjusted according to gene expression analysis.
* Recurrent mutations are defined as mutations at the same amino acid.
** Bonferroni correction was applied to adjust for multiple hypothesis testing.

**Supplemental Table S7. Damaging mutations that occur more often than expected by chance**

| Gene | # of damaging mutations | Adjusted *P* value* |
|---|---|---|
| *TP53* | 18 | 4.39E-45 |
| *CCR4* | 6 | 1.83E-10 |
| *SMARCB1* | 5 | 1.25E-07 |
| *ARID1A* | 7 | 1.36E-07 |
| *TET2* | 7 | 1.60E-07 |
| *CREBBP* | 5 | 1.05E-03 |
| *ZEB1* | 4 | 4.95E-03 |
| *FAS* | 3 | 6.85E-03 |
| *NCOR1* | 4 | 5.62E-02 |

Damaging mutations include splice-site mutations, truncating nonsense mutations, and frameshift mutations.
Rate of background damaging mutations were determined by gene expression analysis. The expected number of damaging mutations per gene was adjusted to gene length.
* Bonferroni correction was applied to adjust for multiple hypothesis testing.

**Supplemental Table S8. Description of T cell lymphoma genetic studies (non-CTCL) used in scheme of RHOA distribution and pan-T cell lymphoma analysis.**

| Study | Patient characterization | # of samples | Sequencing type |
|---|---|---|---|
| Yoo et al *,† [10] | AITL | 5<br>9 | Whole exome*<br>RNAseq† |
| Nagata et al † [11] | ATLL | 203 | Target |
| Vallois et al † [12] | AITL | 72 | Target |
| | PTCL-NOS | 13 | Target |
| Kataoka et al* [13] | ATLL | 81 | Whole exome |
| Sakata-Yanagimoto et al* [14] | AITL, PTCL-NOS | 6 | Whole exome |
| Palomero et al* [15] | AITL, PTCL-NOS, nasal-type NKTCL, EATL | 12 | Whole exome |
| Crescenzo et al* [16] | ALK$^-$ ALCL | 23 | Whole exome |
| Roberti et al* [17] | EATL | 15 | Whole exome |

† Studies and data were used in distribution of RHOA mutations.
* Studies and data were used in pan-T cell lymphoma analysis.
AITL, Angioimmunoblastic T cell lymphoma; ATLL, Adult T-cell leukemia/lymphoma; PTCL-NOS, Peripheral T-cell lymphoma not otherwise specified; ALK$^-$ ALCL, Anaplastic large cell lymphoma without anaplastic lymphoma kinase; nasal-type NKTCL, nasal-type Natural killer/T-cell lymphoma; and EATL, Enteropathy-associated T-cell lymphoma

**Supplemental Table S9. CTCL mutations that are statistically significant hotspot mutations in a pan-T cell lymphoma analysis**

| Gene | Recurrent mutation* | TCL | CTCL | Adjusted *P* value** |
|---|---|---|---|---|
| *CCR4* | p.Y331X; p.Y331N | 12 | 4 | 1.39E-59 |
| *PRKCB* | p.D427N | 15 | 1 | 1.39E-59 |
| *PLCG1* | p.R48W | 11 | 4 | 5.26E-55 |
| *PLCG1* | p.S345F | 4 | 8 | 1.84E-41 |
| *STAT3* | p.Y640F | 9 | 2 | 5.08E-37 |
| *STAT5B* | p.N642H | 5 | 3 | 5.75E-24 |
| *CD28* | p.F51V; p.F51I | 3 | 3 | 1.50E-15 |
| *CARD11* | p.E626K | 5 | 1 | 1.50E-15 |
| *JAK3* | p.A573V | 3 | 2 | 1.87E-11 |
| *SMARCB1* | p.Q368X | 1 | 3 | 1.86E-07 |
| *PLCG1* | p.S520F | 2 | 2 | 1.86E-07 |
| *CSNK1A1* | p.S27F; p.S27C | 2 | 2 | 1.86E-07 |
| *STAT5B* | p.V712E | 3 | 1 | 1.86E-07 |
| *JAK3* | p.M511I | 3 | 1 | 1.86E-07 |
| *CARD11* | p.D401N | 1 | 2 | 1.39E-03 |
| *TRRAP* | p.S722F | 2 | 1 | 1.39E-03 |
| *RARA* | p.G303S | 2 | 1 | 1.39E-03 |

TCL, Number of mutations in T cell lymphomas (other than CTCL). These include ATLL, AITL, PTCL-NOS, EATL, nasal-type NK/T cell lymphoma, $ALK^-$ ALCL.
CTCL, Number of mutations in CTCLs
The list only includes mutations that are also seen in the CTCL cohort.
Rate of background mutations were determined for each gene and adjusted according to gene expression analysis.
* Recurrent mutations are defined as mutations that induce a nonsynonymous amino acid substitution at the same amino acid.
** Bonferroni correction was applied to adjust for multiple hypothesis testing.
; If the same amino acid position is subject to multiple amino acid substitutions, these amino acids are separated by a ;.

**Supplemental Table S10. CTCL mutations in T cell lymphoma oncogenes**

| Gene | Hotspot mutations* |
|---|---|
| *VAV1*[13] | p.R797G;p.R797N, p.R798Q; p.R798P |
| *PRKCB*[13] | p.D427N |
| *JAK3*[17] | p.A573V |
| *STAT5B*[17] | p.N642H |

*List of hotspot mutations shared by CTCL with putative oncogenes in other T cell lymphomas.

**Supplemental Table S11. Damaging mutations in putative tumor suppressors in T cell lymphomas.**

| Gene | Damaging mutations |
|---|---|
| *CD58*[15] | p.S75fs |
| *DNMT3A*[15] | p.W305X, p.Y584X, c.1409_1409delinsTT |

**Supplemental Table S12. CTCL mutations that are hotspot mutations in COSMIC**

| Gene | Amino acid change | # of mutations in COSMIC at amino acid position | Functionally validated | Candidate | Targetable |
|---|---|---|---|---|---|
| *KRAS* | p.G13D | 5057 | Y | | Y |
| *TP53* | p.R273H | 747 | | | |
| *TP53* | p.R248W | 684 | Y | | Y |
| *U2AF1* | p.S34F | 196 | Y | | Y |
| *BRAF* | p.K601E | 140 | Y | | Y |
| *TP53* | p.H179Y | 117 | | | |
| *STAT3* | p.Y640F | 92 | Y | | Y |
| *TP53* | p.P250S | 57 | | | |
| *STAT5B* | p.N642H | 55 | Y | | Y |
| *TP53* | p. R273P | 40 | | | |
| *BRAF* | p.D594N | 39 | Y | | Y |
| *NRAS* | p.G13C | 34 | Y | | Y |
| *TMPRSS13* | p.Q78R | 31 | | | |
| *TMPRSS13* | p.A77G | 31 | | | |
| *TP53* | p.T155N | 30 | | | |
| *PLCG1* | p.S345F | 25 | Y | | Y |
| *JAK3* | p.M511I | 23 | Y | | Y |
| *BCOR** | p.N1425S | 19 | | Y | |
| *TRRAP* | p.S722F | 19 | | | |
| *KRT8* | p.S31A | 18 | | | |
| *JAK3* | p.A573V | 17 | Y | | |
| *QRICH2* | p.G634S | 16 | | | |

| | | | | |
|---|---|---|---|---|
| *MAP2K1*** | p.E203K | 12 | Y | Y |

Y refers to yes

* This amino acid alteration has been reported to be a likely gain-of-function recurrent amino acid alteration in endometrial and uterine carcinomas.[18,19]

** Although there were fewer than 15 instances of *MAP2K1* p.E203K, it has been listed since it is a functionally validated amino acid alteration found in melanomas and lung cancers.[20]

**Supplemental Table S13. Damaging mutations in canonical tumor suppressors**

| Gene | # of damaging mutations |
|---|---|
| *TET2* | 7 |
| *ARID1A* | 6 |
| *KMT2D* | 3 |
| *KDM6A* | 2 |
| *NF1* | 1 |
| *KMT2C* | 1 |
| *PIK3R1* | 1 |

Canonical tumor suppressors reflect the consensus cancer genes[18] wherein >20% of the mutations are damaging mutations in COSMIC.

**Supplemental Table S14. Damaging mutations in recurrent focal deletions.**

| Cytoband | Wide peak boundaries | % of CTCLs with deletions | # of genes in peak | Candidate gene | Candidate gene by damaging mutation burden | # of damaging mutations |
|---|---|---|---|---|---|---|
| 1p36.11 | chr1:26673679-27110886 | 57.50% | 7 | *ARID1A* | ***ARID1A*** | 7 |
| 9p21.3 | chr9:21849450-21996041 | 40.00% | 1 | *CDKN2A** | ***CDKN2A*** | 1 |
| 10p11.22 | chr10:31205853-32136797 | 60.00% | 1 | *ZEB1* | ***ZEB1*** | 4 |
| 10q24.32 | chr10:104131016-104230563 | 67.50% | 7 | *NFKB2* | ***NFKB2*** | 1 |
| 2p23.3 | chr2:24949121-25818354 | 37.50% | 4 | *DNMT3A* | ***DNMT3A*** | 3 |
| 11q22.3 | chr11:107234547-107759139 | 30.00% | 5 | *ATM** | None | NA |
| 2q37.3 | chr2:239018134-242951149 | 20.00% | 38 | *PDCD1* | ***PDCD1*** | 2 |
| 19p13.3 | chr19:1-55701376 | 42.50% | 1078 | *STK11* | *JUNB/NCAN/ZBTB7A* | 2 |
| 9q21.32 | chr9:80386282-90795694 | 32.50% | 33 | *DAPK1* | None | NA |
| 13q14.2 | chr13:47731103-56619937 | 30.00% | 40 | *RB1* | ***SETDB2*** | 1 |
| 19p13.3 | chr19:2029483-3927502 | 32.50% | 53 | *GADD45B* | *ZFR2* | 1 |
| 12p13.2 | chr12:9777007-14468100 | 17.50% | 64 | *CDKN1B* | *CLEC1A* | 1 |
| 6q23.3 | chr6:138243081-138525040 | 25.00% | 2 | *TNFAIP3* | ***TNFAIP3*** | 2 |
| 10q21.2 | chr10:63698286-64053033 | 52.50% | 2 | *ZNF365** | None | NA |
| 10q26.3 | chr10:127512506- | 55.00% | 46 | *MGMT* | *DOCK1* | 1 |

| | | | | | | |
|---|---|---|---|---|---|---|
| | 135374737 | | | | | |
| 7p21.1 | chr7:15566451-36519345 | 27.50% | 107 | *NFE2L3* | *ITGB8/STK31* | 1 |
| 9q31.1 | chr9:96260592-105897449 | 25.00% | 58 | *XPA* | *PLPPR1/TMEM246* | 1 |
| 6q25.2 | chr6:153645511-170899992 | 20.00% | 73 | *CCR6* | *FNDC1* | 2 |
| 12q21.33 | chr12:87113009-111341205 | 20.00% | 160 | *SOCS2* | *NR1H4* | 2 |
| 6q21 | chr6:106661861-112488015 | 17.50% | 42 | *TRAF3IP2* | *FYN/SMPD2* | 1 |
| 16q22.1 | chr16:66074546-66236753 | 15.00% | 2 | *CTCF** | None | NA |
| 10q26.11 | chr10:120779987-124142656 | 55.00% | 19 | *BAG3* | *TACC2* | 2 |
| 10q23.31 | chr10:90763175-90964816 | 40.00% | 2 | *FAS* | ***FAS*** | 3 |
| 11p13 | chr11:31441250-35596790 | 20.00% | 28 | *WT1* | *CAT/CCDC73* | 1 |
| 6q25.1 | chr6:149953508-150112805 | 22.50% | 3 | *LATS1** | None | NA |
| 16q24.2 | chr16:86667813-88154820 | 12.50% | 21 | *BANP* | None | NA |
| 13q12.13 | chr13:1-40031653 | 17.50% | 101 | *BRCA2* | *GPR12/**RFXAP*** | 2 |
| 1p22.1 | chr1:71317019-96960088 | 15.00% | 106 | *RPL5* | *ARHGAP29/BCAR3/SYDE2* | 1 |
| 8p23.1 | chr8:1-146274826 | 40.00% | 644 | *EGR3* | *CHD7/RIMS2/PREX2/CSMD3/UNC5D* | 2 |

Candidate gene refers to previously identified candidate genes.[1]
Candidate genes by damaging mutations refers to the genes harboring the highest number of damaging mutations in each interval. If there are more than one gene in each interval with the same number of damaging mutations, these genes are all listed, separated by a /.

# of damaging mutations indicates the sum of the truncating nonsense mutations, frameshift mutations, and splice-site mutations.
Underlined genes refer to candidate target genes that have been previously shown to be the target gene in those regions because they harbor significantly more localizing mutations than other genes in that interval. Localizing mutations were defined as focal copy number mutations and point mutations.[1]
* refers to genes previously identified by GRAIL analysis to reside on narrow recurrent chromosomal deletions (<20 genes in the confidence interval). *BAG3* was excluded because of the damaging mutation data suggests that *TACC2* may be the target gene of 10q26.11 deletions.
Genes in bold refers to genes with damaging mutations residing on minimal common regions shared by all copy number mutations that overlap with the indicated confidence interval.

**Supplemental Table S15. Recurrent amino acid alterations in recurrent focal amplifications**

| Cytoband | Wide peak boundaries | % of CTCLs with amplifications | # of genes in peak | Candidate gene | Candidate gene by hotspot analysis | # of hotspot mutations |
|---|---|---|---|---|---|---|
| 10p15.1 | chr10:5882522-7245908 | 30.00% | 9 | *PRKCQ** | None | NA |
| 10p12.33 | chr10:15250463-18469816 | 22.50% | 21 | *TRDMT1* | None | NA |
| 7p22.2 | chr7:1-4248090 | 22.50% | 34 | *CARD11* | ***CARD11*** | 5 |
| 9p24.2 | chr9:2612161-5512649 | 12.50% | 20 | *JAK2** | None | NA |
| 6p25.3 | chr6:1-1258328 | 5.00% | 5 | *IRF4* | ***IRF4*** | 2 |
| 7q34 | chr7:127929037-158821424 | 17.50% | 222 | *BRAF* | ***PTPRN2*** | 2 |
| 17q11.2 | chr17:21750215-37983285 | 62.50% | 283 | *STAT5B* | ***STAT5B*** | 3 |

Candidate gene refers to candidate genes identified in a previous analysis.[1]
* refers to genes previously identified by GRAIL analysis to reside on narrow recurrent chromosomal amplifications (<20 genes in the confidence interval).
Bold refers to genes with recurrent amino acid alterations residing in each GISTIC confidence interval.
# of hotspot mutations indicate the number of mutations that occur at the identical amino acid position in the CTCL cohort (n=220 patients).

**Supplemental Table S16. Oncogenic mutations previously functionally validated in CTCL.**

| Genes | Nonsynonymous mutations† |
|---|---|
| *TNFRSF1B* [2] | p.S254C, p.G256C (2), p.F258C, p.T377I |
| *JAK1* [5] | p.R659C, p.L710V |
| *JAK3* [3,5,7] | p.A573V (2), p.M511I (2), p.V678L, p.S989I, p.Y1023H |
| *PLCG1* [4] | p.R48W (4), p.D342N, p.S345F (9), p.S520F (2), p.G772V, p.E989K, p.L1035V, p.E1163K (3) |
| *CARD11* [7] | p.D357A*/E/N, p.M360K, p.Y361C, p.D401N (2), p.A598T*, p.S615F (3), p.E626K, p.R891P |
| *MAPK1* [7] | p.E322A/K (2) |
| *PRKG1* [7] | p.E17K, p.R21Q, p.T298I*, p.T327N*, p.G642E |
| *POT1* [21] | p.V28G, p.F31S, p.S38N, p.T53A*, p.F62I††, p.K90E, p.W148X, p.S270N, p.V434I* |

Underlined mutations were functionally validated in previous CTCL studies.
If the amino acid alterations occur at the same position, each amino acid substitution is separated by a /.
† Numbers in parenthesis indicate number of mutations in CTCL if they were discovered in more than 1 patient.
†† p.F62V was validated.
* Refers to amino acid alterations found only in samples without matched normal controls.

**Supplemental Table S17. Mutations distribution according to patient CTCL subtype in 55 of putative driver genes.**

| Genes | SS (186) # of total mutations | MF (25) # of total mutations | *P* value* |
|---|---|---|---|
| *TP53* | 31 | 1 | 0.137 |
| *PLCG1* | 18 | 4 | 0.306 |
| *CARD11* | 12 | 1 | 1 |
| *ARID1A* | 12 | 3 | 0.399 |
| *TRRAP* | 11 | 0 | 0.369 |
| *POT1* | 10 | 0 | 0.612 |
| *DNMT3A* | 10 | 0 | 0.612 |
| *TET2* | 9 | 0 | 0.603 |
| *RHOA* | 9 | 1 | 1 |
| *CD28* | 8 | 0 | 0.600 |
| *ZEB1* | 8 | 0 | 0.600 |
| *RLTPR* | 7 | 0 | 1 |
| *CREBBP* | 7 | 0 | 1 |
| *NCOR1* | 7 | 0 | 1 |
| *STAT5B* | 7 | 1 | 1 |
| *KMT2D* | 6 | 1 | 0.592 |
| *BCOR* | 6 | 0 | 1 |
| *CCR4* | 6 | 1 | 0.592 |
| *FAS* | 6 | 0 | 1 |
| *KMT2C* | 5 | 0 | 1 |
| *RARA* | 5 | 0 | 1 |
| *TNFRSF1B* | 5 | 0 | 1 |
| *PRKG1* | 4 | 1 | 0.471 |
| *PTPRN2* | 4 | 1 | 0.471 |
| *NFKB2* | 4 | 0 | 1 |
| *ATM* | 3 | 1 | 0.399 |
| *SMARCB1* | 3 | 2 | 0.108 |
| *CTCF* | 3 | 0 | 1 |
| *JAK3* | 3 | 2 | 0.108 |
| *VAV1* | 3 | 1 | 0.399 |
| *NF1* | 3 | 0 | 1 |
| *ZNF365* | 2 | 0 | 1 |
| *IRF4* | 2 | 0 | 1 |
| *PDCD1* | 2 | 0 | 1 |
| *PRKCQ* | 2 | 0 | 1 |

| | | | |
|---|---|---|---|
| *KDM6A* | 2 | 0 | 1 |
| *ARHGEF3* | 2 | 0 | 1 |
| *RFXAP* | 2 | 0 | 1 |
| *CSNK1A1* | 2 | 0 | 1 |
| *TNFAIP3* | 2 | 0 | 1 |
| *PIK3R1* | 2 | 0 | 0.399 |
| *SETDB2* | 1 | 0 | 1 |
| *JAK1* | 1 | 1 | 0.223 |
| *STAT3* | 1 | 1 | 0.223 |
| *CD58* | 1 | 0 | 1 |
| *PRKCB* | 1 | 0 | 1 |
| *BRAF* | 1 | 0 | 1 |
| *KRAS* | 1 | 0 | 1 |
| *NRAS* | 1 | 0 | 1 |
| *LATS1* | 1 | 0 | 1 |
| *U2AF1* | 0 | 1 | 0.119 |
| *MAPK1* | 0 | 3 | 0.001 |
| *MAP2K1* | 0 | 1 | 0.119 |
| *CDKN2A* | 0 | 0 | 1 |
| *JAK2* | 0 | 0 | 1 |

Number in parenthesis represents the number of patients in each CTCL subtype
* *P* value was determined by Fisher's exact test compared between SS and MF.

**Supplemental Table S18. Identification of differentially expressed genes in PMA/ionomycin treated Jurkat cells (RLTPR (p.Q575E) compared to WT RLTPR).**

| | $log_2$ Fold change | *P* value | Adjusted *P* value |
|---|---|---|---|
| *TTC40* | 2.654820607 | 7.07E-29 | 9.57E-25 |
| *IL3* | 1.751125554 | 5.09E-18 | 3.44E-14 |
| *PRG2* | 1.899816619 | 7.87E-16 | 3.55E-12 |
| *LTA* | 1.583531369 | 1.37E-15 | 4.63E-12 |
| *MAF* | -1.63072702 | 7.85E-15 | 2.12E-11 |
| *IL1RL1* | 1.701563936 | 1.70E-12 | 3.84E-09 |
| *CPNE8* | 1.667188189 | 1.33E-11 | 2.38E-08 |
| *STAT5A* | 1.452137765 | 1.41E-11 | 2.38E-08 |
| *ACSL1* | 1.060028015 | 1.29E-10 | 1.93E-07 |
| *TIFA* | 0.979366913 | 1.90E-10 | 2.57E-07 |
| *VCAM1* | 1.499637999 | 2.70E-10 | 3.32E-07 |
| *PRCP* | 1.047945181 | 6.90E-10 | 7.77E-07 |
| *CD83* | 1.058629302 | 9.62E-10 | 9.36E-07 |
| *SNX30* | -0.984386942 | 9.68E-10 | 9.36E-07 |
| *RUNX1* | -1.074634003 | 1.69E-09 | 1.53E-06 |
| *GBP5* | 0.900572153 | 1.98E-09 | 1.67E-06 |
| *ICAM1* | 1.452103943 | 2.81E-09 | 2.23E-06 |
| *SELE* | 1.413677318 | 3.72E-09 | 2.80E-06 |
| *RGCC* | -0.942395782 | 5.93E-09 | 4.22E-06 |
| *TNFSF15* | 1.340778523 | 1.06E-08 | 7.19E-06 |
| *JADE2* | 0.981004298 | 1.59E-08 | 1.03E-05 |
| *LPAR5* | -1.004974551 | 2.84E-08 | 1.73E-05 |
| *TGFBR3* | 1.284304288 | 2.94E-08 | 1.73E-05 |
| *HEG1* | 0.895888749 | 3.81E-08 | 2.15E-05 |
| *KLF2* | -1.24841969 | 4.98E-08 | 2.69E-05 |
| *PTGIR* | 1.325054948 | 5.93E-08 | 3.09E-05 |
| *TNRC6C-AS1* | -0.97784547 | 6.57E-08 | 3.29E-05 |
| *RGS16* | 1.239835572 | 7.13E-08 | 3.45E-05 |
| *FMNL3* | 0.926907075 | 8.28E-08 | 3.86E-05 |
| *PPP4R4* | 1.196556579 | 9.64E-08 | 4.35E-05 |
| *PRKCH* | -0.819690124 | 1.22E-07 | 5.33E-05 |
| *ANP32A* | 0.719242514 | 1.41E-07 | 5.94E-05 |
| *CXCL3* | 1.252553756 | 1.58E-07 | 6.49E-05 |
| *FAM129A* | 1.245653946 | 1.70E-07 | 6.76E-05 |
| *IKBKE* | 0.826769334 | 2.07E-07 | 8.01E-05 |
| *FAS* | 1.006747122 | 2.72E-07 | 9.67E-05 |

| | | | |
|---|---|---|---|
| *NOG* | -1.266716805 | 2.67E-07 | 9.67E-05 |
| *SIGLEC6* | -1.221227256 | 2.70E-07 | 9.67E-05 |
| *ANKH* | -0.70347971 | 3.06E-07 | 0.000104816 |
| *CSF2* | 1.149925905 | 3.16E-07 | 0.000104816 |
| *DENND5A* | 1.069873079 | 3.18E-07 | 0.000104816 |
| *IER5L* | -1.040561759 | 3.62E-07 | 0.000113455 |
| *KCTD11* | -0.963865024 | 3.77E-07 | 0.000113455 |
| *SEMA4D* | -0.740408009 | 3.70E-07 | 0.000113455 |
| *SERPINA1* | 1.242847502 | 3.59E-07 | 0.000113455 |
| *NDST3* | -0.975804322 | 4.16E-07 | 0.000122234 |
| *MMP9* | 1.167954124 | 4.36E-07 | 0.000125448 |
| *SMS* | 0.740734034 | 4.50E-07 | 0.000126901 |
| *EEF1A2* | 0.974633247 | 5.22E-07 | 0.000144144 |
| *LOC101926963* | 1.010619416 | 6.17E-07 | 0.000163968 |
| *SNX11* | 0.816270163 | 6.18E-07 | 0.000163968 |
| *TMC6* | -0.90142964 | 6.86E-07 | 0.000178441 |
| *CD248* | -1.108290592 | 7.27E-07 | 0.000185552 |
| *CADM1* | 0.897947714 | 8.04E-07 | 0.000199282 |
| *CD28* | -0.84902247 | 8.25E-07 | 0.000199282 |
| *IRX5* | 0.778602948 | 8.19E-07 | 0.000199282 |
| *SATB1* | -0.716608889 | 8.87E-07 | 0.000210556 |
| *KIF25-AS1* | 1.204969691 | 9.20E-07 | 0.000214501 |
| *DENND4A* | 0.889738589 | 1.00E-06 | 0.00022975 |
| *JAZF1* | 0.979620038 | 1.06E-06 | 0.000238443 |
| *NCOA7* | 0.85617053 | 1.28E-06 | 0.000283966 |
| *BTBD11* | -0.818906954 | 1.36E-06 | 0.000295781 |
| *NDRG1* | -0.748866107 | 1.38E-06 | 0.000296473 |
| *CBFA2T3* | -0.787686455 | 1.52E-06 | 0.00032032 |
| *IKZF3* | 0.907195093 | 1.87E-06 | 0.000389746 |
| *CHRNA6* | 1.172425398 | 1.95E-06 | 0.000396425 |
| *RHOV* | 1.148852716 | 1.96E-06 | 0.000396425 |
| *CCR4* | 0.856913581 | 2.05E-06 | 0.000407256 |
| *IFIH1* | 0.863423957 | 2.22E-06 | 0.000435067 |
| *TNC* | 1.154784 | 2.57E-06 | 0.000496747 |
| *UBASH3B* | -0.893553282 | 3.21E-06 | 0.000612438 |
| *MICAL2* | -0.747769865 | 3.43E-06 | 0.000636649 |
| *RASGRP1* | 0.847064 | 3.43E-06 | 0.000636649 |
| *TM2D3* | 0.849736646 | 3.54E-06 | 0.000647614 |
| *BCL2L1* | 0.858260994 | 4.33E-06 | 0.000776178 |
| *CXorf40B* | 0.871850323 | 4.36E-06 | 0.000776178 |

| | | | |
|---|---|---|---|
| *CD74* | 1.087615452 | 5.37E-06 | 0.000943083 |
| *UXS1* | 0.979255903 | 5.51E-06 | 0.000955853 |
| *RGS3* | -0.791107441 | 5.66E-06 | 0.000958045 |
| *SHISA2* | -0.843870841 | 5.66E-06 | 0.000958045 |
| *C16orf54* | -0.77719779 | 5.79E-06 | 0.00096765 |
| *CCL1* | 1.084666888 | 6.91E-06 | 0.001139865 |
| *JAM2* | 1.064763303 | 7.29E-06 | 0.001174664 |
| *NHSL2* | 0.972044985 | 7.22E-06 | 0.001174664 |
| *FAM63B* | -0.810618599 | 7.73E-06 | 0.001209838 |
| *MATN2* | 1.066589203 | 7.74E-06 | 0.001209838 |
| *RNF166* | -0.750219299 | 7.78E-06 | 0.001209838 |
| *KCNQ3* | 0.916352369 | 8.67E-06 | 0.001332679 |
| *ITIH5* | 1.087422314 | 1.03E-05 | 0.001560994 |
| *CD40* | 1.038826593 | 1.09E-05 | 0.001636953 |
| *CCDC6* | 0.757551683 | 1.14E-05 | 0.001699865 |
| *ARHGAP31* | 0.829804623 | 1.20E-05 | 0.001761419 |
| *GDF10* | -1.07755773 | 1.23E-05 | 0.001791055 |
| *FOXO1* | 0.757201673 | 1.27E-05 | 0.001835045 |
| *SULT1B1* | -1.03269465 | 1.36E-05 | 0.001939766 |
| *TNF* | 0.943851305 | 1.39E-05 | 0.001954196 |
| *ATP8B3* | -0.745605385 | 1.55E-05 | 0.002161567 |

Differential gene expression was determined by DESeq2 with default settings.
For sake of clarity, top 100 genes by adjusted *P* value are shown.

**Supplemental Table S19. Identification of differentially expressed genes in unstimulated Jurkat cells (RLTPR (p.Q575E) compared to WT RLTPR)**

| | $log_2$ Fold change | *P* value | Adjusted *P* value |
|---|---|---|---|
| *RMRP* | 0.048039 | 0.031401 | 0.999999 |
| *RPPH1* | 0.039435 | 0.041014 | 0.999999 |
| *THOC7-AS1* | 0.024926 | 0.060702 | 0.999999 |
| *LSP1* | -0.091245 | 0.063349 | 0.999999 |
| *ONECUT1* | 0.090442 | 0.072623 | 0.999999 |
| *CDH4* | -0.091964 | 0.078526 | 0.999999 |
| *AGRP* | -0.018412 | 0.084164 | 0.999999 |
| *EPHB2* | -0.093191 | 0.084799 | 0.999999 |
| *HCCAT3* | -0.018294 | 0.085070 | 0.999999 |
| *GAA* | -0.105849 | 0.086630 | 0.999999 |
| *FAM188B* | -0.017929 | 0.088298 | 0.999999 |
| *PDGFRB* | -0.054604 | 0.088662 | 0.999999 |
| *ISM1* | 0.094224 | 0.089461 | 0.999999 |
| *GJC3* | -0.021092 | 0.089963 | 0.999999 |
| *IFIH1* | 0.100018 | 0.094374 | 0.999999 |
| *SNORA15* | -0.022560 | 0.095599 | 0.999999 |
| *NEFL* | 0.064962 | 0.098413 | 0.999999 |
| *NOX1* | 0.061767 | 0.098779 | 0.999999 |
| *NPPA-AS1* | -0.040710 | 0.099489 | 0.999999 |

Differential gene expression was determined by DESeq2 with default settings.
We show genes with a *P* value of < 0.1. No genes had an adjusted P value < 0.99999.

**Supplemental Table S20. Identification of differentially expressed genes in RLTPR (p.Q575E) overexpressed Jurkat cells after PMA/Ionomycin treatment.**

| | $log_2$ Fold change | *P* value | Adjusted *P* value |
|---|---|---|---|
| *TNF* | 6.70845 | 7.81E-137 | 1.22E-132 |
| *BCL2A1* | 8.26175 | 1.63E-127 | 8.51E-124 |
| *EGR1* | 7.14825 | 1.59E-127 | 8.51E-124 |
| *CD69* | 6.97668 | 4.38E-123 | 1.71E-119 |
| *NR4A1* | 5.29725 | 2.92E-114 | 9.14E-111 |
| *IL2RA* | 5.80012 | 1.77E-108 | 4.60E-105 |
| *CSF2* | 8.23231 | 1.33E-106 | 2.97E-103 |
| *IL3* | 8.29212 | 2.70E-106 | 5.27E-103 |
| *LTB* | 6.06968 | 2.81E-105 | 4.87E-102 |
| *CCL4* | 8.48354 | 8.04E-105 | 1.26E-101 |
| *EGR3* | 6.95425 | 3.03E-102 | 4.31E-99 |
| *IL21R* | 6.78811 | 1.84E-97 | 2.39E-94 |
| *CD83* | 3.54276 | 3.05E-97 | 3.67E-94 |
| *NFKBIA* | 4.17087 | 3.06E-95 | 3.42E-92 |
| *BIRC3* | 4.69011 | 1.78E-93 | 1.85E-90 |
| *XCL1* | 7.90832 | 1.44E-92 | 1.41E-89 |
| *NR4A3* | 6.03418 | 5.02E-90 | 4.61E-87 |
| *RGS16* | 6.32293 | 1.34E-85 | 1.16E-82 |
| *CXCL8* | 7.99861 | 2.19E-85 | 1.80E-82 |
| *EGR2* | 6.25338 | 4.74E-83 | 3.71E-80 |
| *DUSP2* | 4.78691 | 2.99E-82 | 2.22E-79 |
| *IER3* | 4.63580 | 3.75E-81 | 2.66E-78 |
| *CCL3* | 8.00003 | 4.27E-77 | 2.90E-74 |
| *LTA* | 6.23422 | 8.07E-77 | 5.25E-74 |
| *RELB* | 4.77533 | 8.72E-76 | 5.45E-73 |
| *TRAF1* | 5.31246 | 1.15E-74 | 6.90E-72 |
| *GBP5* | 3.98982 | 1.56E-74 | 9.05E-72 |
| *ARHGAP31* | 3.68127 | 3.06E-73 | 1.71E-70 |
| *CCL20* | 7.39828 | 2.81E-72 | 1.52E-69 |
| *XCL2* | 5.88155 | 1.78E-69 | 9.29E-67 |
| *NFKB2* | 4.34810 | 1.88E-69 | 9.45E-67 |
| *ZFP36L1* | 3.68835 | 1.10E-66 | 5.37E-64 |
| *C3* | 7.08505 | 6.55E-65 | 3.10E-62 |
| *CRTAM* | 6.73619 | 9.18E-65 | 4.22E-62 |
| *HIVEP3* | 2.95764 | 9.98E-65 | 4.46E-62 |
| *TRIB1* | 5.00000 | 4.57E-64 | 1.98E-61 |

| | | | |
|---|---|---|---|
| *STAT5A* | 3.87977 | 1.16E-63 | 4.91E-61 |
| *IL18R1* | 4.99447 | 2.21E-63 | 9.09E-61 |
| *VCAM1* | 7.18410 | 7.13E-62 | 2.86E-59 |
| *IL4I1* | 6.43485 | 1.03E-61 | 4.02E-59 |
| *SPRY4* | 3.85151 | 2.64E-61 | 1.01E-58 |
| *BCL6* | 3.99510 | 1.51E-60 | 5.61E-58 |
| *TNFRSF9* | 7.16964 | 1.03E-57 | 3.75E-55 |
| *PMEPA1* | -3.73913 | 2.59E-57 | 9.20E-55 |
| *BTG2* | 3.54986 | 2.31E-55 | 8.02E-53 |
| *MMP9* | 4.84347 | 3.47E-55 | 1.18E-52 |
| *STAT4* | 3.55837 | 5.77E-55 | 1.92E-52 |
| *MB* | 6.53428 | 1.91E-54 | 6.22E-52 |
| *TNFRSF18* | 4.28284 | 7.94E-54 | 2.53E-51 |
| *SERINC5* | -2.70573 | 9.31E-54 | 2.91E-51 |
| *REL* | 3.38231 | 2.87E-53 | 8.78E-51 |
| *TNFSF15* | 4.73944 | 1.09E-52 | 3.28E-50 |
| *HCAR1* | 6.17348 | 1.29E-52 | 3.81E-50 |
| *TNFSF14* | 5.87970 | 2.04E-51 | 5.89E-49 |
| *BTG1* | 3.19480 | 1.50E-50 | 4.27E-48 |
| *LOC101926963* | 4.10806 | 2.64E-49 | 7.36E-47 |
| *PDGFA* | 3.01825 | 3.56E-49 | 9.77E-47 |
| *DUSP10* | 4.01449 | 2.26E-48 | 6.08E-46 |
| *ZC3H12A* | 3.00353 | 5.07E-48 | 1.34E-45 |
| *ITK* | 2.86256 | 1.90E-46 | 4.96E-44 |
| *MYO7B* | -2.88877 | 7.75E-45 | 1.99E-42 |
| *SDC4* | 6.27169 | 4.87E-43 | 1.23E-40 |
| *EVI2A* | 3.26092 | 8.39E-43 | 2.08E-40 |
| *ENTPD2* | 4.85369 | 2.51E-42 | 6.12E-40 |
| *HIVEP2* | 2.74772 | 4.44E-42 | 1.07E-39 |
| *MYEOV* | 6.09105 | 2.25E-41 | 5.33E-39 |
| *CCND1* | 2.95279 | 3.67E-41 | 8.57E-39 |
| *EBI3* | 6.24157 | 7.46E-41 | 1.69E-38 |
| *TTC40* | 5.77296 | 7.47E-41 | 1.69E-38 |
| *PHLDA1* | 3.00623 | 9.80E-41 | 2.19E-38 |
| *NFKB1* | 2.53821 | 1.01E-40 | 2.22E-38 |
| *EDARADD* | 2.74617 | 2.19E-40 | 4.76E-38 |
| *TNFRSF4* | 3.57407 | 8.96E-40 | 1.92E-37 |
| *TNFAIP3* | 3.43137 | 1.24E-39 | 2.62E-37 |
| *TGFBR3* | 4.59799 | 4.91E-39 | 1.02E-36 |
| *RUNX1* | -2.21553 | 5.21E-39 | 1.07E-36 |

| | | | |
|---|---|---|---|
| *SELPLG* | -3.79431 | 1.02E-38 | 2.06E-36 |
| *POU2F2* | 2.79719 | 4.00E-38 | 8.01E-36 |
| *PPP1R16B* | 2.88067 | 2.63E-37 | 5.20E-35 |
| *CMPK2* | -2.36334 | 7.88E-37 | 1.54E-34 |
| *PRSS35* | 5.61465 | 1.40E-36 | 2.71E-34 |
| *LYST* | 2.59715 | 2.75E-36 | 5.24E-34 |
| *APOBEC3G* | 3.23661 | 4.07E-36 | 7.66E-34 |
| *DUSP6* | 3.88445 | 4.35E-35 | 8.09E-33 |
| *RHOU* | -2.84376 | 8.43E-35 | 1.55E-32 |
| *SGK1* | 3.43098 | 2.24E-34 | 4.06E-32 |
| *CDKN1A* | 2.88453 | 3.46E-34 | 6.15E-32 |
| *NCEH1* | 2.25343 | 3.47E-34 | 6.15E-32 |
| *3-Sep* | -2.53890 | 9.49E-34 | 1.67E-31 |
| *ZFP36L2* | -2.20856 | 4.74E-33 | 8.23E-31 |
| *BCL2L11* | 2.34703 | 9.09E-33 | 1.56E-30 |
| *NOTCH3* | -2.77119 | 9.58E-33 | 1.63E-30 |
| *LRRC8B* | 2.24462 | 1.30E-32 | 2.19E-30 |
| *RAB3D* | -2.53979 | 1.77E-32 | 2.93E-30 |
| *GPR17* | -4.07111 | 2.82E-32 | 4.59E-30 |
| *JAM2* | 3.95967 | 2.82E-32 | 4.59E-30 |
| *SDCBP* | 2.01415 | 5.30E-32 | 8.54E-30 |

Unstimulated RLTPR (p.Q575E) Jurkat cells represent the controls.
Differential gene expression was determined by DESeq2 with default settings.
We show genes with adjusted *P* value of $< 0.1$
For sake of clarity, top 100 genes by adjusted *P* value are shown.

**Supplemental Table S21. Identification of differentially expressed genes in RLTPR WT overexpressed Jurkat cells after PMA/Ionomycin treatment.**

| | $log_2$ Fold change | *P* value | Adjusted *P* value |
|---|---|---|---|
| *EGR1* | 7.722852929 | 2.14E-264 | 3.36E-260 |
| *CD69* | 6.597143158 | 4.97E-183 | 3.89E-179 |
| *HIVEP3* | 3.169956207 | 3.12E-172 | 1.63E-168 |
| *EGR3* | 8.027018541 | 1.71E-156 | 6.70E-153 |
| *EGR2* | 7.034406276 | 3.46E-108 | 1.08E-104 |
| *SLA* | 2.512935553 | 7.03E-108 | 1.83E-104 |
| *GBP5* | 3.14173557 | 1.62E-96 | 3.62E-93 |
| *TRIB1* | 5.114136437 | 1.98E-93 | 3.88E-90 |
| *PMEPA1* | -3.922808957 | 1.16E-90 | 2.01E-87 |
| *DUSP2* | 4.372912312 | 1.80E-89 | 2.82E-86 |
| *ST8SIA4* | 2.545889055 | 4.02E-84 | 5.72E-81 |
| *PPP3CA* | 2.317481813 | 4.08E-79 | 5.33E-76 |
| *CXCL8* | 6.656973869 | 5.54E-78 | 6.67E-75 |
| *XCL1* | 6.795614701 | 2.22E-74 | 2.48E-71 |
| *DUSP6* | 4.105458933 | 5.34E-70 | 5.58E-67 |
| *IER2* | 2.424165228 | 8.56E-69 | 8.37E-66 |
| *ZFP36L1* | 3.802236181 | 5.49E-67 | 5.06E-64 |
| *PPP1R16B* | 3.085261616 | 2.62E-64 | 2.28E-61 |
| *ITK* | 2.596810294 | 1.09E-62 | 8.96E-60 |
| *RELB* | 4.118973891 | 2.98E-62 | 2.33E-59 |
| *IER3* | 4.305634904 | 1.71E-61 | 1.28E-58 |
| *CRTAM* | 5.795501563 | 2.69E-59 | 1.92E-56 |
| *PVRL1* | -1.885891494 | 3.63E-59 | 2.47E-56 |
| *SLC2A3* | 2.837613853 | 5.99E-59 | 3.91E-56 |
| *CCL1* | 4.43770143 | 2.46E-56 | 1.54E-53 |
| *ZFP36L2* | -2.109825935 | 1.23E-55 | 7.42E-53 |
| *MAF* | 3.347610408 | 1.89E-54 | 1.10E-51 |
| *EDARADD* | 2.582715276 | 3.73E-53 | 2.09E-50 |
| *CLEC2B* | 2.858364982 | 4.37E-52 | 2.28E-49 |
| *NTRK1* | 3.906090317 | 4.24E-52 | 2.28E-49 |
| *IL3* | 5.70050141 | 2.65E-51 | 1.34E-48 |
| *SPRY4* | 3.901056063 | 1.41E-48 | 6.88E-46 |
| *LTA* | 3.995204166 | 1.57E-46 | 7.47E-44 |
| *LRP10* | 1.862461378 | 2.45E-46 | 1.13E-43 |
| *HCAR1* | 5.606736208 | 8.38E-46 | 3.75E-43 |
| *NFKB2* | 3.32958761 | 3.43E-45 | 1.49E-42 |

| | | | |
|---|---|---|---|
| *ACSL6* | -2.206043955 | 5.33E-45 | 2.26E-42 |
| *CCL4* | 5.809360867 | 7.10E-45 | 2.93E-42 |
| *XBP1* | 1.379486305 | 8.62E-45 | 3.46E-42 |
| *GCNT4* | 2.44027959 | 7.64E-44 | 2.99E-41 |
| *NKD2* | -2.557511117 | 1.62E-43 | 6.19E-41 |
| *NFATC1* | 1.920326795 | 2.73E-43 | 1.02E-40 |
| *FAM53B* | -1.731632049 | 7.26E-43 | 2.64E-40 |
| *RAB3D* | -2.302226261 | 1.76E-42 | 6.27E-40 |
| *TNFSF14* | 5.106800149 | 2.64E-42 | 9.19E-40 |
| *IL4I1* | 4.954427177 | 6.60E-42 | 2.25E-39 |
| *HIVEP2* | 2.545743285 | 1.43E-41 | 4.75E-39 |
| *LRRC8B* | 2.202781931 | 5.02E-39 | 1.64E-36 |
| *BCL11B* | -2.137726782 | 5.81E-39 | 1.86E-36 |
| *ENTPD2* | 4.459343085 | 8.01E-39 | 2.51E-36 |
| *PTGER4* | 1.789752889 | 1.12E-38 | 3.43E-36 |
| *EVI2A* | 3.473087699 | 2.06E-38 | 6.20E-36 |
| *CD83* | 2.362950194 | 1.27E-37 | 3.76E-35 |
| *MICAL2* | 2.446154151 | 1.32E-37 | 3.83E-35 |
| *JUNB* | 2.217467166 | 2.24E-37 | 6.38E-35 |
| *MPZL3* | 2.17016195 | 2.73E-37 | 7.63E-35 |
| *FOS* | 3.859043711 | 8.34E-37 | 2.29E-34 |
| *PER1* | 1.397162318 | 2.01E-36 | 5.44E-34 |
| *EGR4* | 4.554262216 | 1.13E-35 | 2.99E-33 |
| *SLAMF6* | 1.654978216 | 1.71E-35 | 4.48E-33 |
| *DNAJB11* | 1.515501285 | 2.33E-35 | 5.97E-33 |
| *TGFBR2* | 2.47138998 | 4.09E-35 | 1.03E-32 |
| *MGAT4A* | -1.680920438 | 4.77E-35 | 1.19E-32 |
| *RLTPR* | 2.505532029 | 8.60E-35 | 2.10E-32 |
| *HUNK* | -1.958991455 | 1.25E-34 | 3.01E-32 |
| *APOBEC3G* | 2.612466748 | 2.69E-34 | 6.38E-32 |
| *LAX1* | 1.996622806 | 5.22E-34 | 1.22E-31 |
| *SEC31B* | -1.581721922 | 5.80E-34 | 1.34E-31 |
| *HBEGF* | 2.795123692 | 6.34E-34 | 1.44E-31 |
| *3-Sep* | -2.0821549 | 7.41E-34 | 1.66E-31 |
| *RAB8B* | 1.831090788 | 1.08E-33 | 2.38E-31 |
| *ELF1* | 1.370574493 | 1.23E-33 | 2.67E-31 |
| *PRDM8* | 2.617216221 | 1.95E-33 | 4.18E-31 |
| *SOX12* | -1.777218518 | 2.39E-33 | 5.06E-31 |
| *HRH2* | 4.984817208 | 2.71E-33 | 5.66E-31 |
| *GPR84* | 2.515651042 | 7.66E-33 | 1.58E-30 |

| | | | |
|---|---|---|---|
| *SFMBT2* | 1.831898276 | 1.63E-32 | 3.32E-30 |
| *HIRA* | -1.306735985 | 2.24E-32 | 4.49E-30 |
| *MUC2* | 4.925215776 | 5.25E-32 | 1.04E-29 |
| *ARHGAP31* | 2.599465732 | 7.84E-32 | 1.54E-29 |
| *OCSTAMP* | 4.862994163 | 1.47E-31 | 2.84E-29 |
| *PITX1* | -1.825411034 | 3.24E-31 | 6.20E-29 |
| *SH2B3* | 1.926008632 | 6.54E-31 | 1.23E-28 |
| *EDEM1* | 1.338296998 | 6.81E-31 | 1.27E-28 |
| *DNAJC3* | 1.641629573 | 7.11E-31 | 1.31E-28 |
| *NAB2* | 2.314508257 | 8.74E-31 | 1.59E-28 |
| *C3* | 4.915256885 | 1.52E-30 | 2.73E-28 |
| *UCK2* | -1.353127591 | 1.54E-30 | 2.74E-28 |
| *CSF2* | 5.093062632 | 2.45E-30 | 4.31E-28 |
| *HDC* | 1.862777823 | 2.76E-30 | 4.81E-28 |
| *PHLDA1* | 3.029881363 | 2.93E-30 | 5.05E-28 |
| *BCL7A* | -1.326482376 | 3.99E-30 | 6.79E-28 |
| *SNX30* | 2.001379888 | 6.08E-30 | 1.02E-27 |
| *SERINC5* | -1.996358265 | 6.84E-30 | 1.14E-27 |
| *ARHGEF3* | 1.786189583 | 7.86E-30 | 1.30E-27 |
| *MYEOV* | 4.719966489 | 8.12E-30 | 1.33E-27 |
| *SGK1* | 2.697082414 | 8.92E-30 | 1.44E-27 |

Unstimulated Jurkat cells expressing WT RLTPR represent the controls.
Differential gene expression was determined by DESeq2 with default settings.
We show genes with adjusted *P* value of $< 0.1$
For sake of clarity, top 100 genes by adjusted *P* value are shown.

**Supplemental Table S22. Gene set enrichment analysis of RLTPR (p.Q575E) overexpressed Jurkat cells after PMA/Ionomycin activation compared to wild type.**

| | logFC | AveExpr | *P* value | Adjusted *P* value |
|---|---|---|---|---|
| HINATA_NFKB_IMMU_INF | 1.028 | 0.028 | 1.42E-06 | 2.68E-04 |
| ESC_V6.5_UP_EARLY.V1_UP | -0.426 | 0.009 | 1.35E-03 | 1.28E-01 |
| PRC2_EDD_UP.V1_UP | -0.494 | 0.010 | 2.89E-03 | 1.82E-01 |
| KRAS.LUNG_UP.V1_DN | -0.369 | 0.007 | 6.60E-03 | 2.46E-01 |
| CSR_EARLY_UP.V1_UP | 0.384 | 0.003 | 7.29E-03 | 2.46E-01 |
| ESC_J1_UP_EARLY.V1_UP | -0.364 | 0.007 | 8.58E-03 | 2.46E-01 |
| RB_P130_DN.V1_DN | 0.369 | -0.022 | 1.34E-02 | 2.46E-01 |
| KRAS.AMP.LUNG_UP.V1_DN | -0.317 | 0.034 | 1.50E-02 | 2.46E-01 |
| KRAS.600.LUNG.BREAST_UP.V1_DN | -0.315 | 0.017 | 1.64E-02 | 2.46E-01 |
| KRAS.PROSTATE_UP.V1_UP | -0.303 | 0.005 | 1.85E-02 | 2.46E-01 |
| BCAT_GDS748_UP | -0.343 | -0.044 | 1.91E-02 | 2.46E-01 |
| ALK_DN.V1_DN | -0.332 | -0.009 | 1.94E-02 | 2.46E-01 |
| IL2_UP.V1_DN | -0.296 | -0.011 | 1.94E-02 | 2.46E-01 |
| SRC_UP.V1_UP | -0.334 | 0.016 | 2.08E-02 | 2.46E-01 |
| BCAT.100_UP.V1_DN | -0.363 | 0.001 | 2.09E-02 | 2.46E-01 |
| ERB2_UP.V1_DN | 0.407 | -0.056 | 2.14E-02 | 2.46E-01 |
| KRAS.LUNG.BREAST_UP.V1_DN | -0.297 | 0.025 | 2.30E-02 | 2.46E-01 |
| PRC1_BMI_UP.V1_UP | -0.281 | 0.014 | 2.45E-02 | 2.46E-01 |
| SIRNA_EIF4GI_DN | 0.352 | -0.042 | 2.49E-02 | 2.46E-01 |
| CAHOY_ASTROCYTIC | 0.275 | -0.008 | 2.60E-02 | 2.46E-01 |
| PIGF_UP.V1_DN | -0.313 | 0.008 | 2.78E-02 | 2.50E-01 |
| LTE2_UP.V1_DN | 0.285 | -0.025 | 3.19E-02 | 2.74E-01 |
| ESC_V6.5_UP_LATE.V1_UP | -0.288 | -0.009 | 3.41E-02 | 2.75E-01 |
| GCNP_SHH_UP_LATE.V1_DN | -0.304 | 0.027 | 3.49E-02 | 2.75E-01 |
| NOTCH_DN.V1_DN | -0.276 | -0.012 | 3.75E-02 | 2.83E-01 |
| PIGF_UP.V1_UP | 0.380 | -0.039 | 4.28E-02 | 3.11E-01 |
| E2F3_UP.V1_UP | -0.331 | 0.015 | 4.56E-02 | 3.19E-01 |
| LEF1_UP.V1_UP | -0.257 | 0.002 | 5.04E-02 | 3.40E-01 |
| ERB2_UP.V1_UP | -0.230 | 0.002 | 5.28E-02 | 3.44E-01 |
| NOTCH_DN.V1_UP | -0.243 | 0.005 | 5.76E-02 | 3.57E-01 |
| CRX_NRL_DN.V1_UP | -0.237 | -0.004 | 5.85E-02 | 3.57E-01 |
| PDGF_ERK_DN.V1_DN | -0.265 | 0.042 | 6.38E-02 | 3.61E-01 |
| KRAS.PROSTATE_UP.V1_DN | -0.226 | 0.011 | 6.72E-02 | 3.61E-01 |
| RAPA_EARLY_UP.V1_UP | -0.238 | 0.018 | 6.75E-02 | 3.61E-01 |
| IL15_UP.V1_DN | -0.214 | 0.005 | 7.07E-02 | 3.61E-01 |

| | | | | |
|---|---|---|---|---|
| BCAT_BILD_ET_AL_UP | -0.301 | -0.007 | 7.17E-02 | 3.61E-01 |
| SNF5_DN.V1_DN | -0.210 | -0.013 | 7.20E-02 | 3.61E-01 |
| WNT_UP.V1_UP | -0.229 | 0.036 | 7.34E-02 | 3.61E-01 |
| MYC_UP.V1_UP | 0.361 | 0.008 | 7.44E-02 | 3.61E-01 |
| PKCA_DN.V1_UP | -0.221 | -0.010 | 7.66E-02 | 3.62E-01 |
| ESC_J1_UP_LATE.V1_UP | -0.212 | -0.002 | 8.32E-02 | 3.82E-01 |
| CAHOY_OLIGODENDROCUTIC | -0.205 | 0.015 | 8.48E-02 | 3.82E-01 |
| PTEN_DN.V2_DN | -0.207 | 0.008 | 9.39E-02 | 3.85E-01 |
| KRAS.BREAST_UP.V1_DN | -0.236 | -0.011 | 9.47E-02 | 3.85E-01 |
| STK33_NOMO_UP | 0.299 | 0.002 | 9.49E-02 | 3.85E-01 |
| CAHOY_ASTROGLIAL | -0.196 | 0.001 | 9.60E-02 | 3.85E-01 |
| CRX_DN.V1_UP | -0.195 | -0.014 | 9.61E-02 | 3.85E-01 |
| RAPA_EARLY_UP.V1_DN | -0.217 | 0.010 | 1.02E-01 | 3.85E-01 |
| GLI1_UP.V1_UP | 0.208 | -0.048 | 1.03E-01 | 3.85E-01 |
| JNK_DN.V1_DN | -0.209 | 0.006 | 1.05E-01 | 3.85E-01 |
| PRC2_EZH2_UP.V1_UP | -0.233 | -0.018 | 1.06E-01 | 3.85E-01 |
| MTOR_UP.V1_UP | -0.208 | 0.011 | 1.06E-01 | 3.85E-01 |
| ATF2_UP.V1_UP | -0.214 | 0.001 | 1.10E-01 | 3.89E-01 |
| GCNP_SHH_UP_LATE.V1_UP | 0.258 | -0.038 | 1.11E-01 | 3.89E-01 |
| CYCLIN_D1_UP.V1_UP | -0.267 | 0.008 | 1.19E-01 | 4.05E-01 |
| GLI1_UP.V1_DN | -0.219 | -0.016 | 1.20E-01 | 4.05E-01 |
| NRL_DN.V1_UP | -0.186 | 0.007 | 1.24E-01 | 4.07E-01 |
| BRCA1_DN.V1_DN | -0.189 | -0.017 | 1.25E-01 | 4.07E-01 |
| MEK_UP.V1_DN | 0.223 | -0.026 | 1.28E-01 | 4.08E-01 |
| MTOR_UP.N4.V1_DN | -0.238 | -0.015 | 1.31E-01 | 4.12E-01 |
| STK33_UP | 0.276 | 0.006 | 1.35E-01 | 4.19E-01 |
| BMI1_DN_MEL18_DN.V1_DN | -0.182 | -0.027 | 1.39E-01 | 4.22E-01 |
| PRC2_SUZ12_UP.V1_UP | -0.176 | -0.002 | 1.43E-01 | 4.22E-01 |
| VEGF_A_UP.V1_DN | 0.256 | -0.047 | 1.44E-01 | 4.22E-01 |
| GCNP_SHH_UP_EARLY.V1_DN | -0.165 | -0.003 | 1.45E-01 | 4.22E-01 |
| IL21_UP.V1_UP | -0.209 | 0.012 | 1.49E-01 | 4.26E-01 |
| P53_DN.V2_DN | -0.172 | -0.012 | 1.51E-01 | 4.26E-01 |
| DCA_UP.V1_UP | -0.167 | -0.011 | 1.60E-01 | 4.26E-01 |
| MYC_UP.V1_DN | -0.166 | -0.013 | 1.60E-01 | 4.26E-01 |
| EGFR_UP.V1_UP | 0.198 | 0.002 | 1.61E-01 | 4.26E-01 |
| KRAS.300_UP.V1_DN | -0.196 | 0.001 | 1.62E-01 | 4.26E-01 |
| SINGH_KRAS_DEPENDENCY_SIGNATURE_ | -0.246 | 0.037 | 1.62E-01 | 4.26E-01 |
| IL21_UP.V1_DN | -0.164 | 0.022 | 1.65E-01 | 4.27E-01 |
| RB_P107_DN.V1_UP | -0.312 | 0.006 | 1.74E-01 | 4.40E-01 |
| BCAT.100_UP.V1_UP | -0.174 | 0.004 | 1.75E-01 | 4.40E-01 |

| | | | | |
|---|---|---|---|---|
| TBK1.DF_DN | 0.230 | -0.021 | 1.80E-01 | 4.48E-01 |
| PKCA_DN.V1_DN | -0.156 | 0.031 | 1.83E-01 | 4.50E-01 |
| MTOR_UP.V1_DN | -0.171 | 0.017 | 1.92E-01 | 4.59E-01 |
| TBK1.DN.48HRS_DN | 0.155 | 0.060 | 1.92E-01 | 4.59E-01 |
| STK33_SKM_UP | 0.194 | -0.019 | 1.96E-01 | 4.59E-01 |
| GCNP_SHH_UP_EARLY.V1_UP | 0.186 | -0.029 | 1.97E-01 | 4.59E-01 |
| P53_DN.V1_DN | -0.155 | -0.002 | 2.05E-01 | 4.73E-01 |
| AKT_UP.V1_DN | -0.157 | 0.010 | 2.10E-01 | 4.77E-01 |
| MTOR_UP.N4.V1_UP | 0.153 | -0.027 | 2.17E-01 | 4.89E-01 |
| ESC_J1_UP_LATE.V1_DN | 0.152 | -0.019 | 2.23E-01 | 4.93E-01 |
| KRAS.600_UP.V1_DN | -0.156 | 0.019 | 2.25E-01 | 4.93E-01 |
| BMI1_DN.V1_DN | -0.156 | -0.013 | 2.27E-01 | 4.93E-01 |
| ATM_DN.V1_UP | -0.158 | -0.006 | 2.41E-01 | 5.15E-01 |
| CSR_LATE_UP.V1_DN | -0.135 | 0.017 | 2.42E-01 | 5.15E-01 |
| LEF1_UP.V1_DN | -0.144 | 0.009 | 2.54E-01 | 5.33E-01 |
| RAF_UP.V1_DN | 0.132 | -0.002 | 2.72E-01 | 5.64E-01 |
| BCAT_GDS748_DN | -0.155 | -0.011 | 2.80E-01 | 5.64E-01 |
| ATF2_S_UP.V1_DN | -0.137 | 0.000 | 2.81E-01 | 5.64E-01 |
| MEK_UP.V1_UP | -0.129 | -0.001 | 2.82E-01 | 5.64E-01 |
| SRC_UP.V1_DN | -0.139 | -0.024 | 2.84E-01 | 5.64E-01 |
| VEGF_A_UP.V1_UP | -0.146 | 0.014 | 2.89E-01 | 5.64E-01 |
| CSR_EARLY_UP.V1_DN | -0.132 | -0.020 | 2.90E-01 | 5.64E-01 |

**Supplemental Table S23. Identification of enriched transcription factor binding sites in genes upregulated in RLTPR (p.Q575E) overexpressed Jurkat cells compared to WT after PMA/Ionomycin treatment.**

| Transcription factor | JASPAR ID | Target gene hits | Target gene non-hits | Back-ground gene hits | Back-ground Gene non-hits | Adjusted *P* value |
|---|---|---|---|---|---|---|
| RELA | MA0107.1 | 56 | 31 | 7171 | 17581 | 1.50E-09 |
| NFKB1 | MA0105.1 | 36 | 51 | 3946 | 20806 | 8.58E-07 |
| NF-kappaB | MA0061.1 | 53 | 34 | 8381 | 16371 | 1.20E-05 |
| REL | MA0101.1 | 60 | 27 | 10514 | 14238 | 2.90E-05 |
| ELK1 | MA0028.1 | 69 | 18 | 13642 | 11110 | 8.72E-05 |
| ELF5 | MA0136.1 | 77 | 10 | 16547 | 8205 | 1.05E-04 |
| GABPA | MA0062.2 | 54 | 33 | 9355 | 15397 | 1.05E-04 |
| SPIB | MA0081.1 | 79 | 8 | 17547 | 7205 | 1.87E-04 |
| SPI1 | MA0080.2 | 74 | 13 | 15792 | 8960 | 1.87E-04 |
| NFE2L2 | MA0150.1 | 38 | 49 | 5635 | 19117 | 1.87E-04 |
| CEBPA | MA0102.2 | 65 | 22 | 12828 | 11924 | 2.13E-04 |
| FEV | MA0156.1 | 72 | 15 | 15402 | 9350 | 4.58E-04 |
| MZF1_5-13 | MA0057.1 | 66 | 21 | 13425 | 11327 | 4.58E-04 |
| EBF1 | MA0154.1 | 58 | 29 | 11288 | 13464 | 7.35E-04 |
| Gfi | MA0038.1 | 66 | 21 | 13731 | 11021 | 9.82E-04 |
| NFATC2 | MA0152.1 | 70 | 17 | 15176 | 9576 | 1.13E-03 |
| TBP | MA0108.2 | 54 | 33 | 10389 | 14363 | 1.28E-03 |
| Hand1::Tcfe2a | MA0092.1 | 64 | 23 | 13286 | 11466 | 1.35E-03 |
| STAT1 | MA0137.2 | 38 | 49 | 6394 | 18358 | 1.96E-03 |
| Nkx2-5 | MA0063.1 | 74 | 13 | 16973 | 7779 | 2.75E-03 |
| HOXA5 | MA0158.1 | 76 | 11 | 17629 | 7123 | 2.75E-03 |

**Supplemental Figure S1. 6 approaches to identify the putative driver genes in CTCL.**

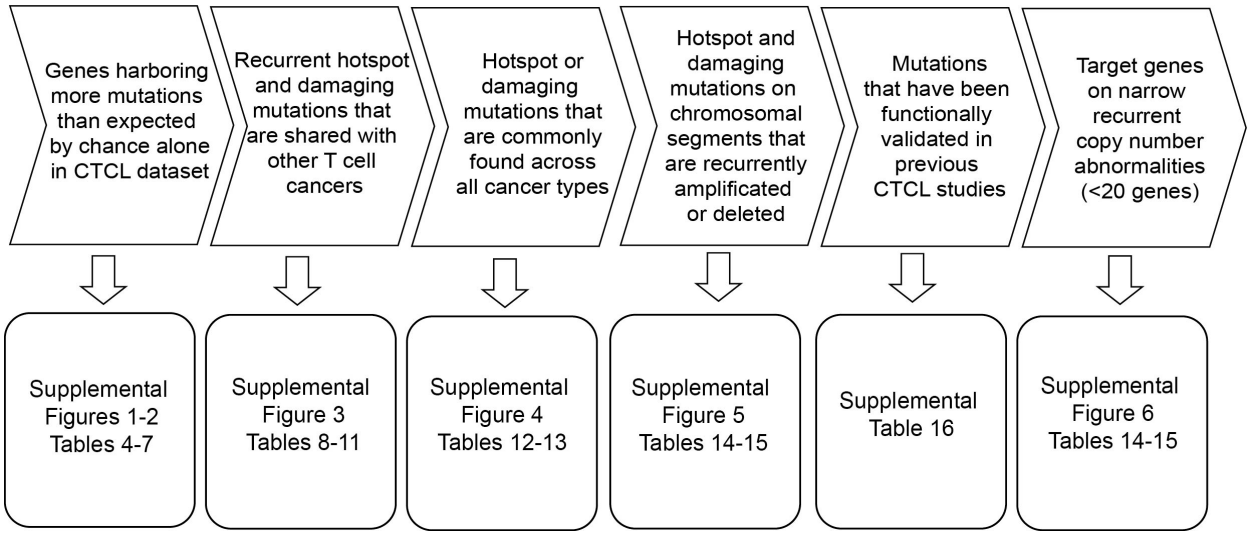


**Supplemental Figure S1.** 6 approaches to identify the putative driver genes in CTCL.

**Supplemental Figure S2. Identification of genes with a statistically significant burden of somatic point mutations.**

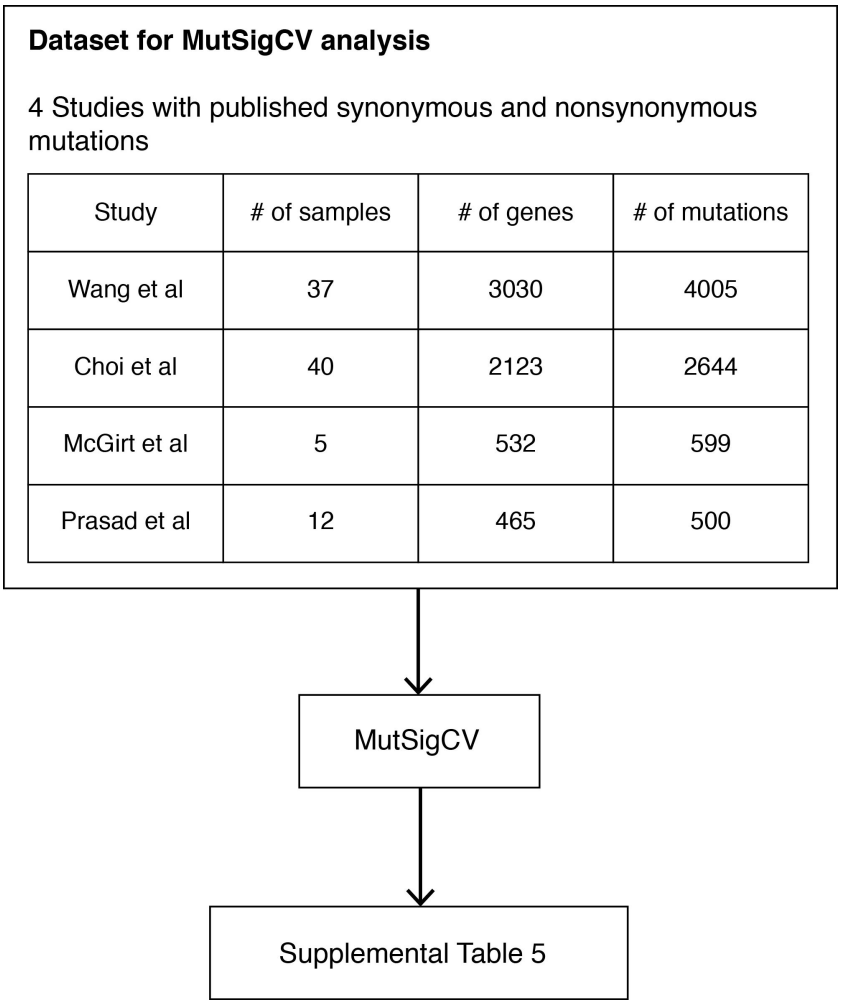


**Supplemental Figure S2**. Identification of genes with a statistically significant burden of somatic point mutations. Tumors from 94 patients across four studies were annotated with both nonsynonymous and synonymous mutations. These data were subject to MutSigCV analysis. The results are reported in supplemental Table 5. For the gene expression covariate, we utilized previously published RNA-seq data.[1]

**Supplemental Figure S3. Identification of putative driver genes with mutational signatures characteristic of oncogenes and tumor suppressors.**

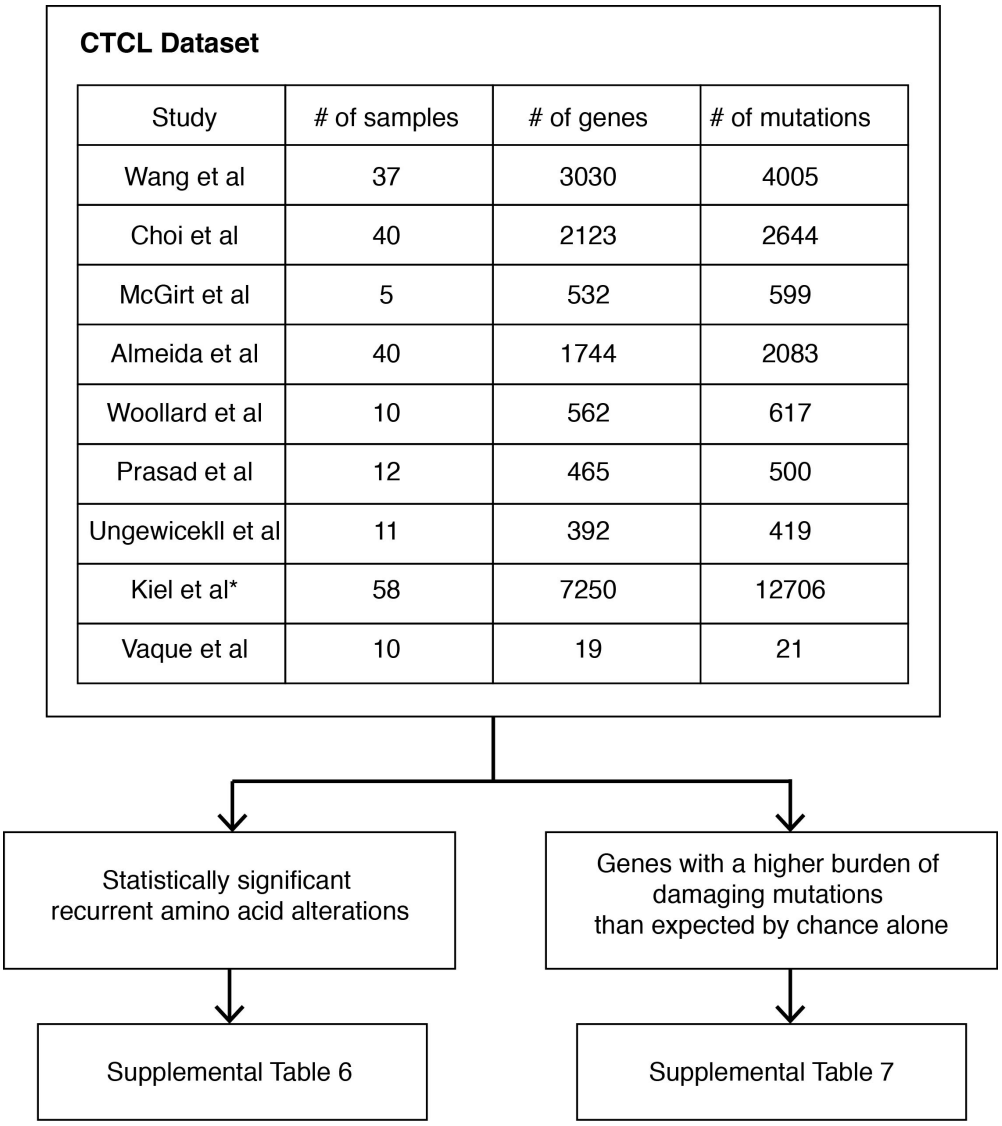


**Supplemental Figure S3**. Identification of putative driver genes with mutational signatures characteristic of oncogenes and tumor suppressors. We identified 1) statistically significant recurrent amino acid alterations and 2) damaging mutations used previously published algorithms.[1,22] For this analysis, we controlled for gene expression and for gene length. *This study did not have germline controls. All samples were filtered for common germline variants which are likely to be false positive and unlikely to contribute to cancer pathogenesis. For this study, we included only missense mutations if they were seen in other studies. All damaging mutations were included in the analysis.

**Supplemental Figure S4. Identification of putative driver gene mutations found in other mature T cell lymphomas.**

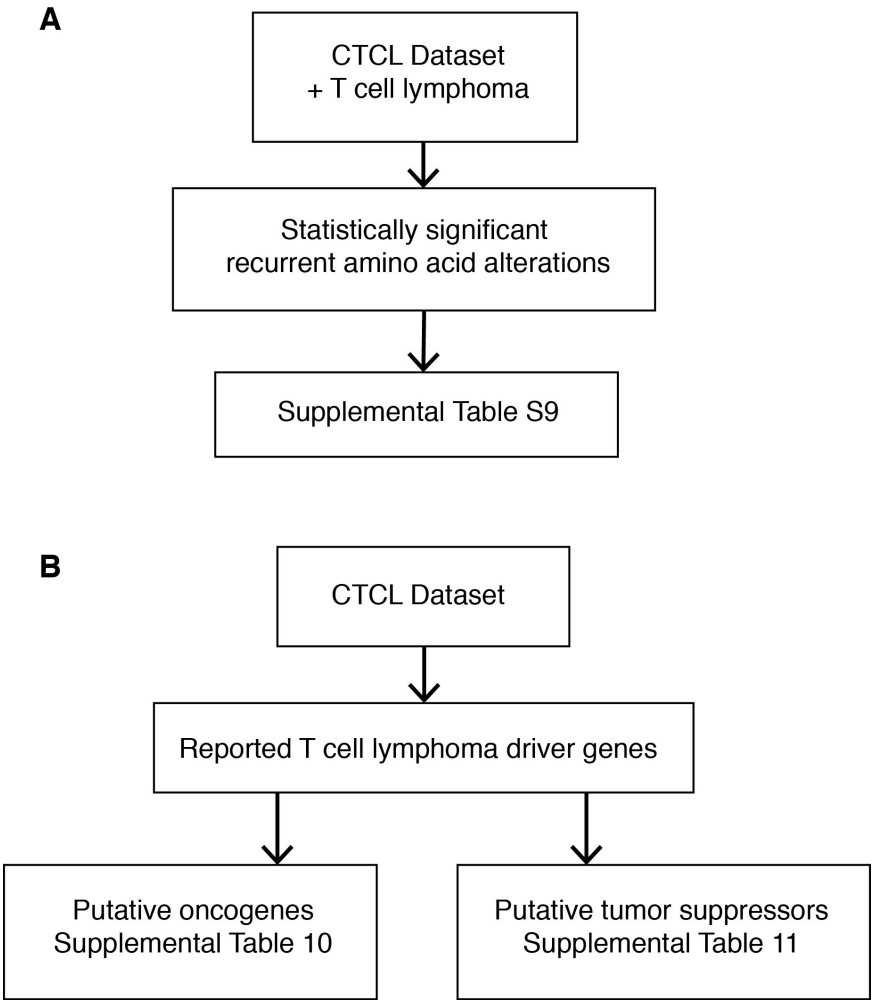


**Supplemental Figure S4.** Identification of putative driver gene mutations found in other mature T cell lymphomas. (A) We performed a pan-T cell lymphoma analysis to identify all recurrent amino acid alterations that occurred more often than expected by chance alone. (B) We specifically queried our dataset for mutations in previously reported driver genes identified in other cancers. For putative oncogenes, we looked for amino acid alterations that are found in hotspots identified in other cancer types. For putative tumor suppressors, we looked for damaging mutations in our CTCL dataset.

**Supplemental Figure S5. Identification of CTCL mutations in consensus cancer genes.**

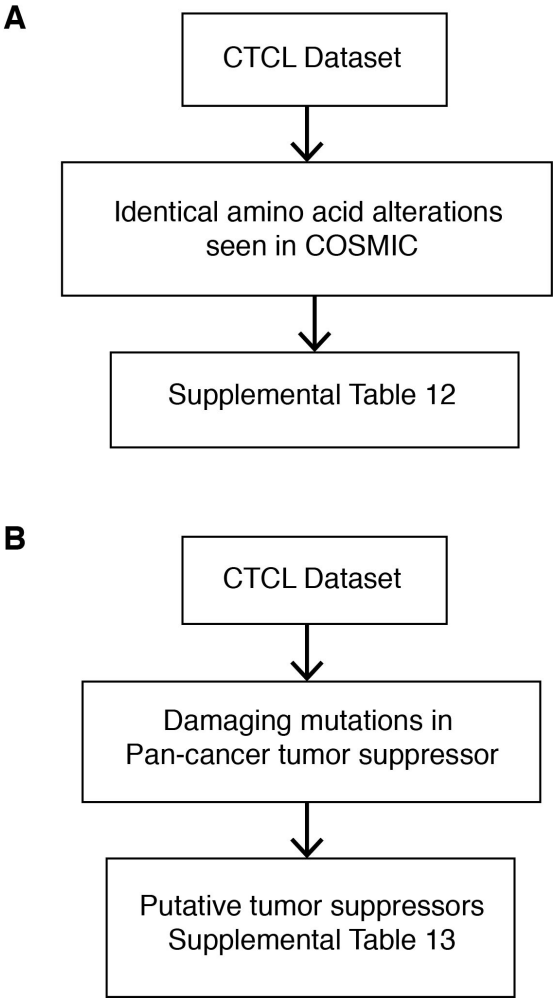


**Supplemental Figure S5.** Identification of CTCL mutations in consensus cancer genes. (A) We looked for recurrent amino acid alterations in putative oncogenes by cross-referencing our CTCL dataset with mutations found in COSMIC. (B) We looked for damaging mutations in consensus cancer genes. We examined the genes determined to be pan-cancer genes.[18] We filtered these genes that harbor damaging mutations in >20% of samples, which is consistent with the consensus signature for tumor suppressors.[22] We report damaging mutations in these genes from the CTCL dataset.

**Supplemental Figure S6. Identification of genes with mutational signatures characteristic of oncogenes and tumor suppressors on recurrent copy number variants.**

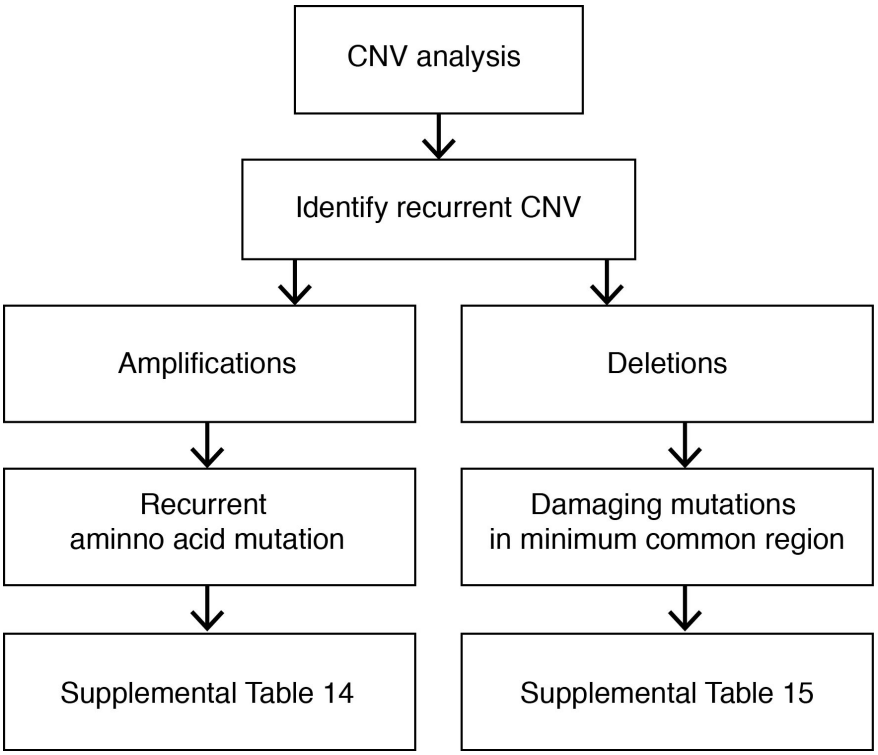


**Supplemental Figure S6.** Identification of genes with mutational signatures characteristic of oncogenes and tumor suppressors on recurrent copy number variants (CNV). We analyzed the statistically significant copy number abnormalities we identified previously.[1] We queried recurrent amplifications for genes with recurrent amino acid alterations, which are characteristic of oncogenes. We queried recurrent deletions for damaging mutations that occurred in genes that reside on the minimal common regions common by CNVs, which are characteristic of tumor suppressors in CTCL.

**Supplemental Figure S7. Identification of target genes on narrow recurrent copy number variants.**

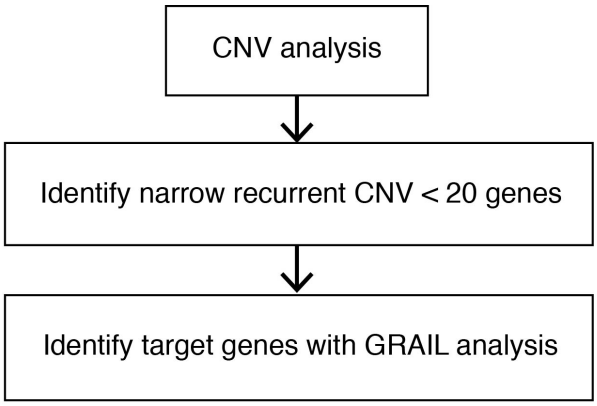


**Supplemental Figure S7.** Identification of target genes on narrow recurrent copy number variants. We include here the genes that have been implicated previously on narrow copy number abnormalities using CNV data from previous study.[1] (fewer than 20 genes in the 90% confidence intervals).

**Supplemental Figure S8. Distribution of Mutations in CTCL**

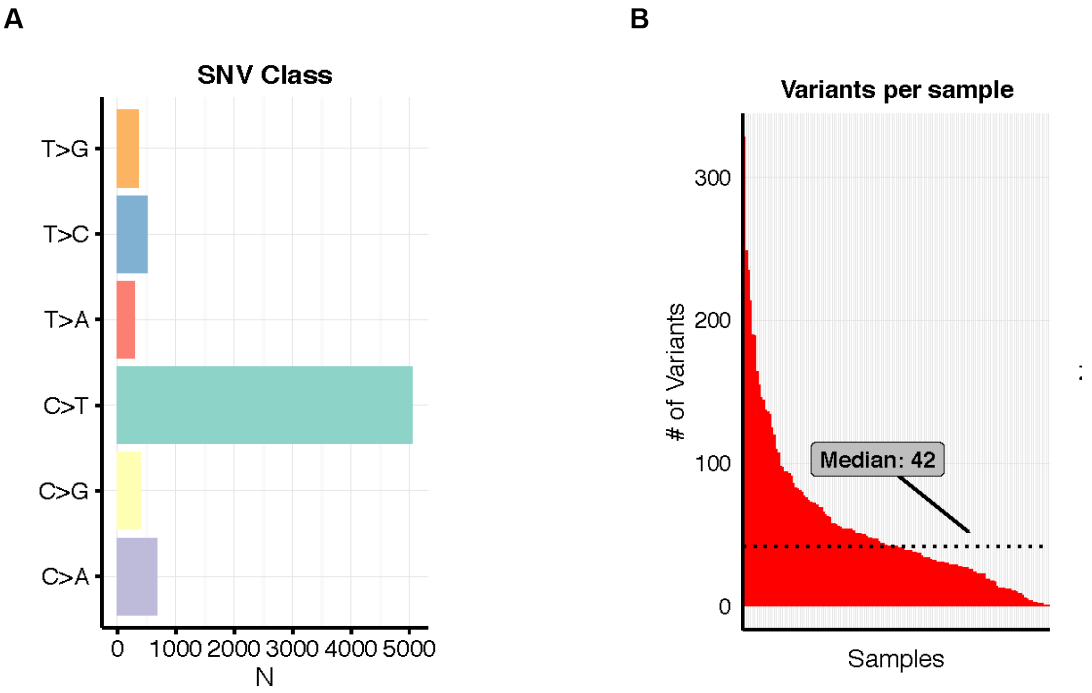


**Supplemental Figure S8.** Distribution of mutations in CTCL. (A) The distribution of mutations by transitions and transversions. (B) The distribution of nonsynonymous variants per sample.

**Supplemental Figure S9. Mapping of RHOA mutations found in T cell lymphomas**

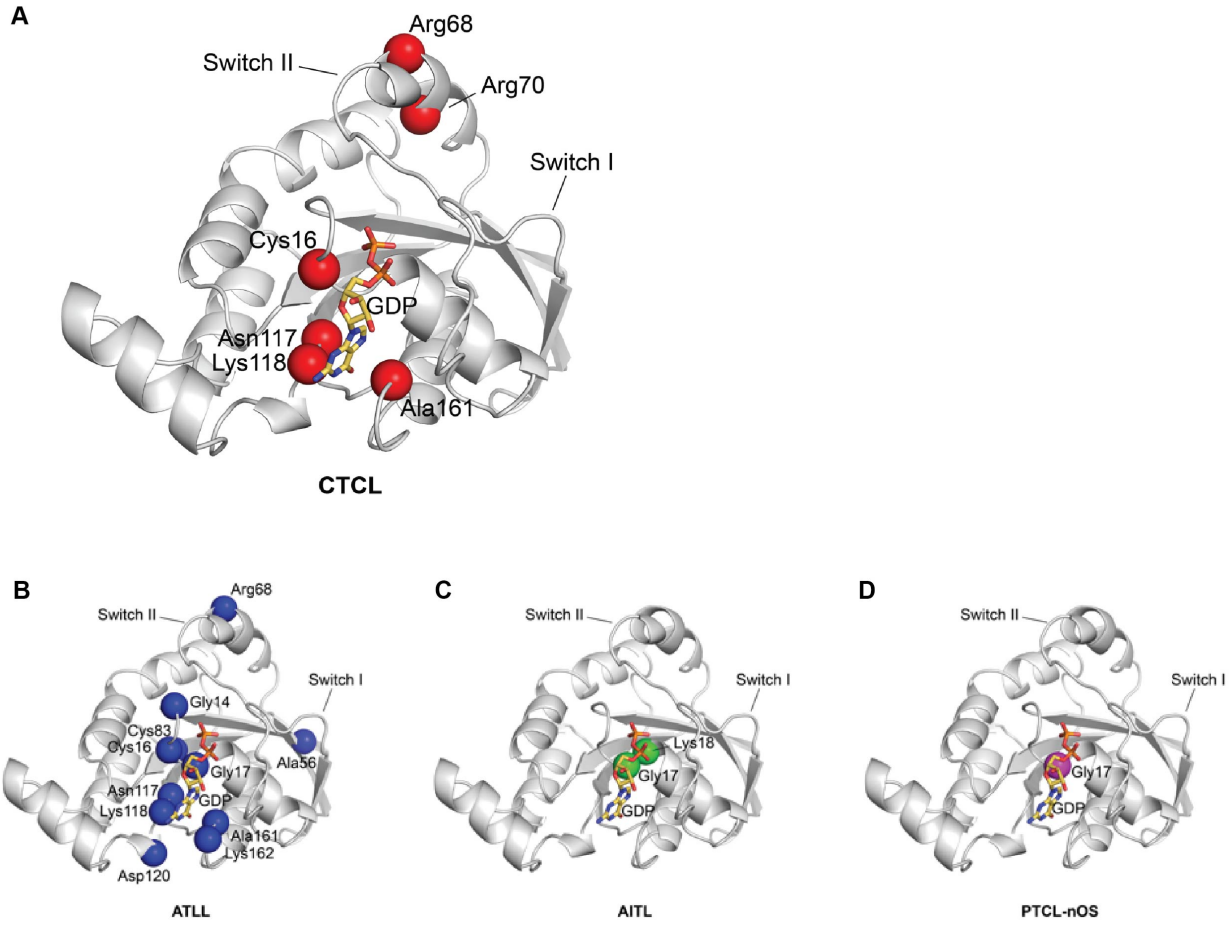


**Supplemental Figure S9.** Mapping of RHOA mutations found in T cell lymphomas. (A) CTCL mutations mapped onto the structure of RHOA in complex with GDP[23] (PDB ID: 1FTN). Switch I and Switch II loops indicated and GDP shown in stick format. (B-D) ATL, AITL and PTCL-NOS mutations mapped onto the structure of RHOA in complex with GDP[23] (PDB ID: 1FTN). Switch I and Switch II loops indicated and GDP shown in stick format.

**Supplemental Figure S10. Lentiviral transduction of Jurkat cells with lentivirus expressing wild-type CK1α, CK1α (p.S27C), or CK1α (p.S27F).**

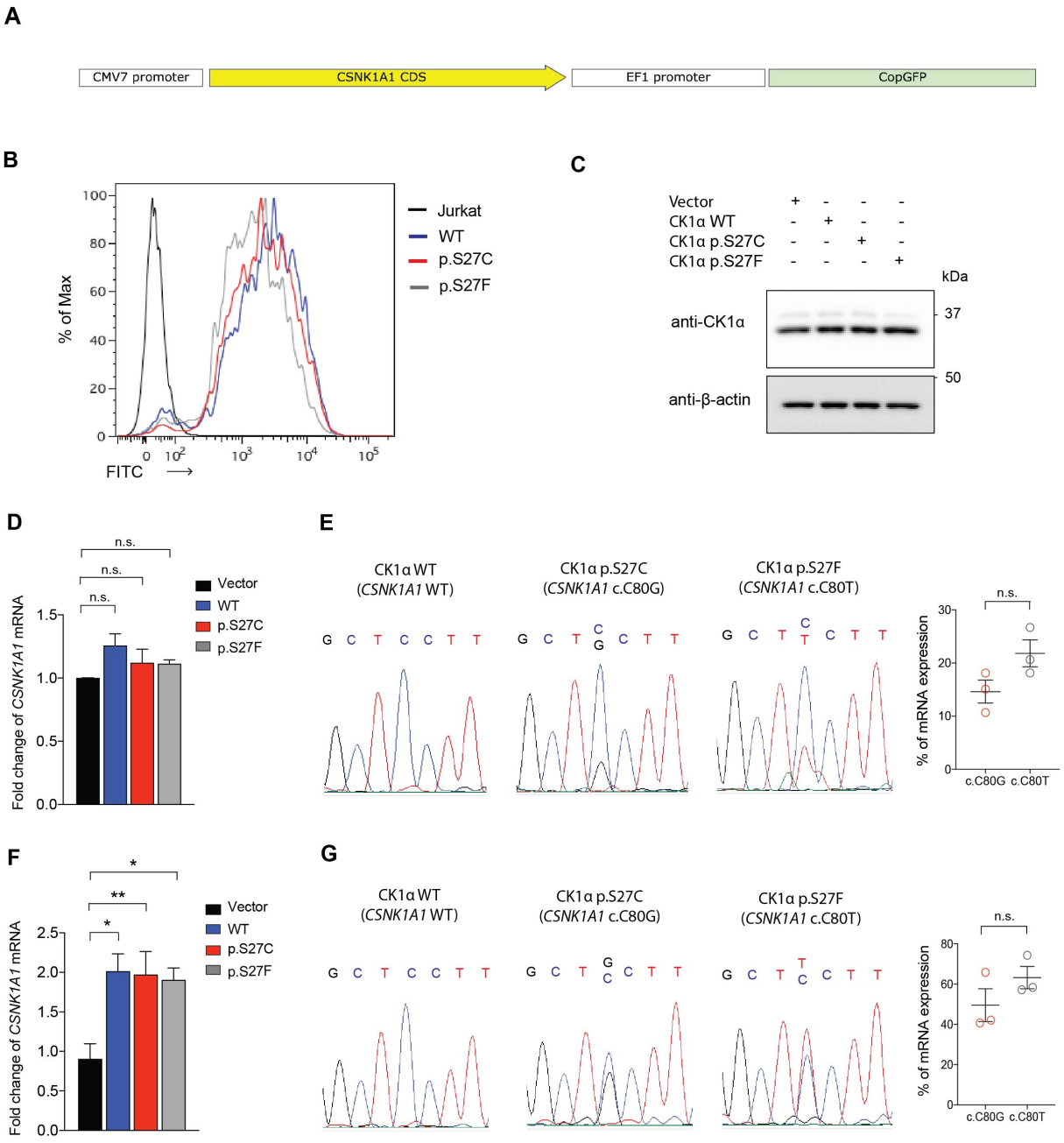


**Supplemental Figure S10.** Lentiviral transduction of Jurkat cells with lentivirus expressing wild-type CK1α, CK1α (p.S27C), or CK1α (p.S27F). (A) Vector map of pCDH-CMV-CSNK1A1-EF1-copGFP. Lentivirally transduced cells express CK1α from the Cytomegalovirus (CMV) promoter and copepod green fluorescent protein (copGFP) from elongation factor 1α (EF1) promoter. (B) Lentivirally transduced cells were selected by sorting for cells expressing copGFP. Post-sort FACS analysis of transduced

Jurkat cells shows uniform copGFP expression. Untransduced Jurkat cells were used as negative control for the absence of copGFP fluorescence. (C) Western blot analysis reveals roughly equivalent expression of CK1$\alpha$ across Jurkat cells, suggesting most of the CK1$\alpha$ protein is derived from the endogenous gene locus and not from the lentivirus. $\beta$-actin is the loading control. Jurkat cells transduced with an empty vector served as the control. (D) qPCR confirms that *CSNK1A1* mRNA levels are similar across Jurkat cohorts, suggesting lentiviral expression of *CSNK1A1* is a fraction of endogenous *CSNK1A1* transcript levels. *P* value was determined by two-sided ratio paired t-test (n.s., not significant). (E) Sanger sequencing of cDNA suggest that only 15 to 26% of the *CSNK1A1* mRNA is the mutant isoform, which is encoded by the lentivirus. The remainder is the wild-type isoform, which is transcribed from the endogenous *CSNK1A1* locus. *P* value was determined by two-sided ratio paired t-test (n.s., not significant). (F) The *CSNK1A1* mRNA is uniformly upregulated by treatment for 6 hours with PMA/ionomycin, a known inducer of CMV promoter.[24] These data show equivalent transcription from lentiviruses in each of the Jurkat cohorts. Jurkat cells transduced with an empty vector served as the control. *P* value was determined by two-sided ratio paired t-test (*$P < .05$, ***$P < .001$). (G) Sanger sequencing reveals that 40 to 74% of the *CSNK1A1* mRNA in PMA/ionomycin stimulated cells is the mutant isoforms, which are encoded by the lentivirus. These data confirm that mRNA induced by PMA/ionomycin is derived from the lentivirus. *P* value was determined by two-sided ratio paired t-test (n.s., not significant).

**Supplemental Figure S11. Identification of a novel RLTPR isoform in human CD4+ T and CTCL cells.**

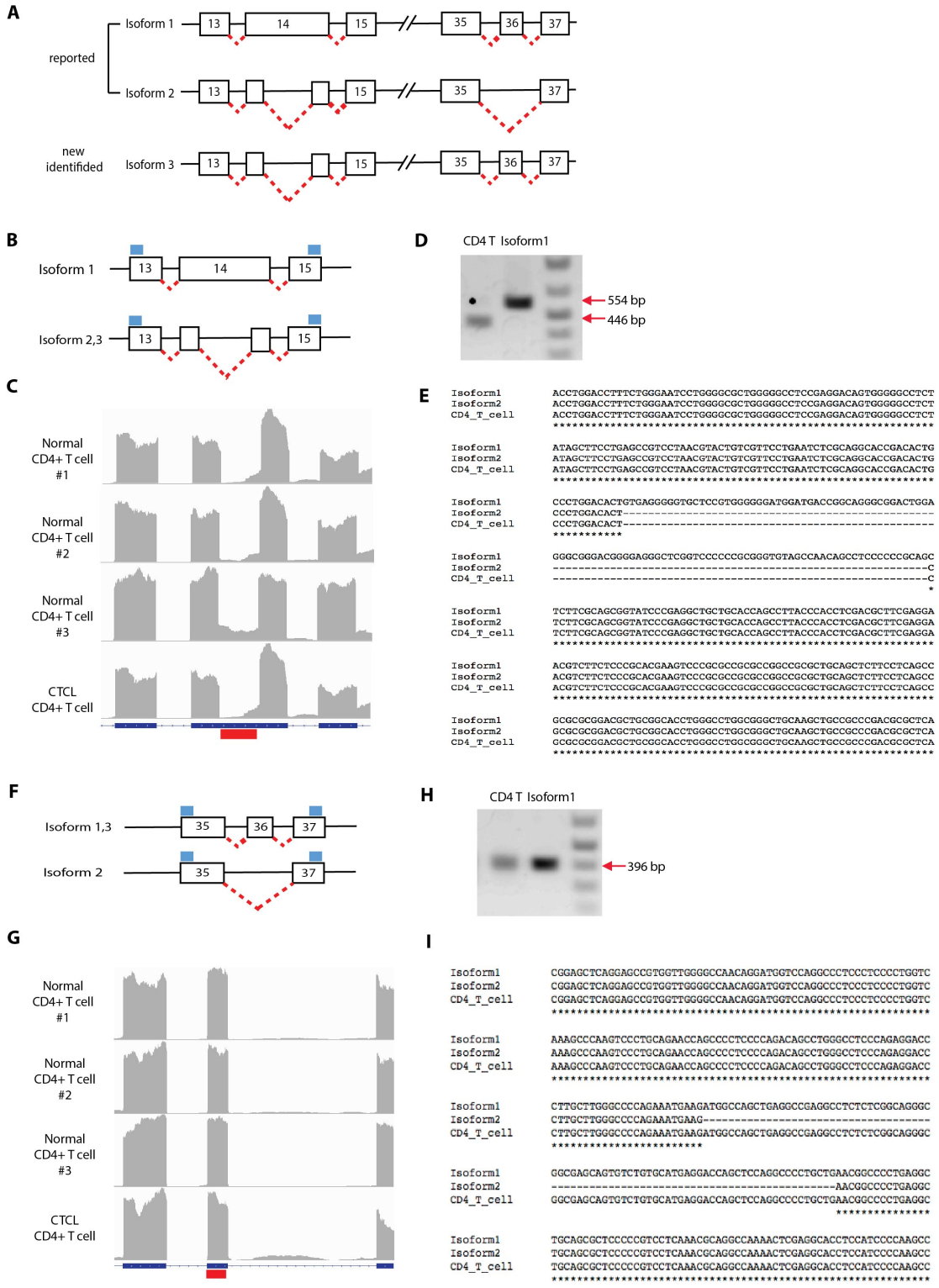

**Supplemental Figure S11**. Identification of a novel RLTPR isoform in human CD4+ T and CTCL cells. (A) Schematics of previously reported and a newly identified isoform in CD4+ T cells and CTCL cells. Each box represents exon and red dotted lines represent alternative splicing. (B) Schematic of each isoform around exon 14. Red dotted lines represent splicing events and blue bar represent the intron-spanning primers designed to amplify the region for gel electrophoresis (D) and Sanger sequencing (E). (C) Integrated genome viewer (IGV) plots of exon 14 from RNAseq of CD4+ T cells from three healthy donors and CTCL tumor cells. The red bar represents the absence of reads aligning to the indicated internal region of exon14. (D) Gel electrophoresis represents amplified PCR segment using cDNA from cDNA of isolated CD4+ T cells and primers indicated in (B). (E) Alignment of the Sanger sequencing results of RLTPR cDNA from CD4 T cells, highlighting that exon14 of new identified isoform is identical with isoform 2 which skips the central portion of exon 14. (E) Schematic of each isoform around exon 36. Red dotted lines represent splicing events and blue bar represent the intron-spanning primers designed to amplify the region for gel electrophoresis (H) and sanger sequencing (I). (G) IGV plots of exon 36 from RNAseq of CTCL cells and CD4+ T cells from three healthy controls. The red bar represents read alignments that map to exon 36. (H) Gel electrophoresis represents amplified PCR segment using cDNA from cDNA of isolated CD4+ T cells and primers indicated in (F). (I) Alignment of the Sanger sequencing results of RLTPR cDNA from CD4 T cells, highlighting that the new identified isoform has exon 36 which is identical with isoform 1.

**Supplemental Figure S12. Volcano plot analysis of RNA expression in Jurkat cells with and without stimulation by the TCR pharmacological mimics (PMA/ionomycin).**

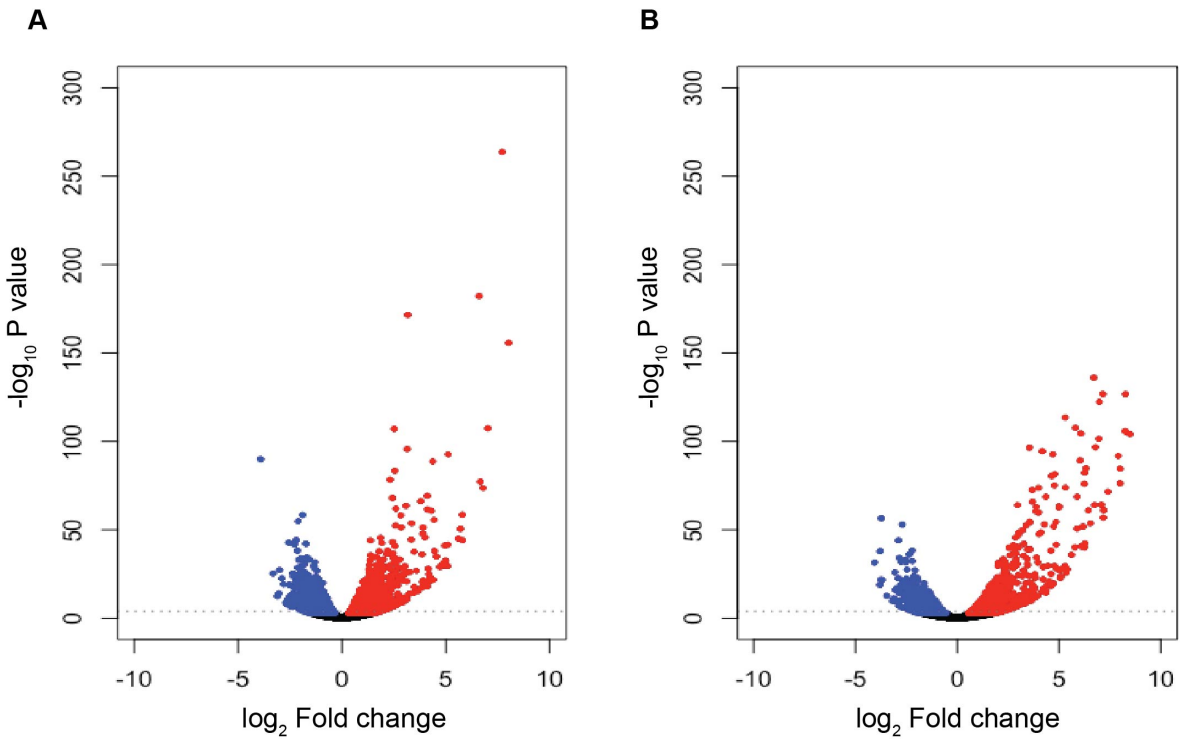


**Supplemental Figure S12**. Volcano plot analysis of RNA expression in Jurkat cells with and without stimulation by the TCR pharmacological mimics (PMA/ionomycin). We show the volcano plots highlighting the DESeq2 results from stimulated RLTPR WT Jurkat (A) and RLTPR (p.Q575E) Jurkats compared to unstimulated controls, respectively (B). Dots which are above gray dotted line represent statistically significant events with adjusted *P* value less than 0.01. Red and blue dots represent upregulated and downregulated genes respectively.

**Supplemental Figure S13. OPOSSUM Analysis for detection of over-represented conserved transcription factor binding sites at promoters of genes upregulated in stimulated RLTPR (p.Q575E) cells.**

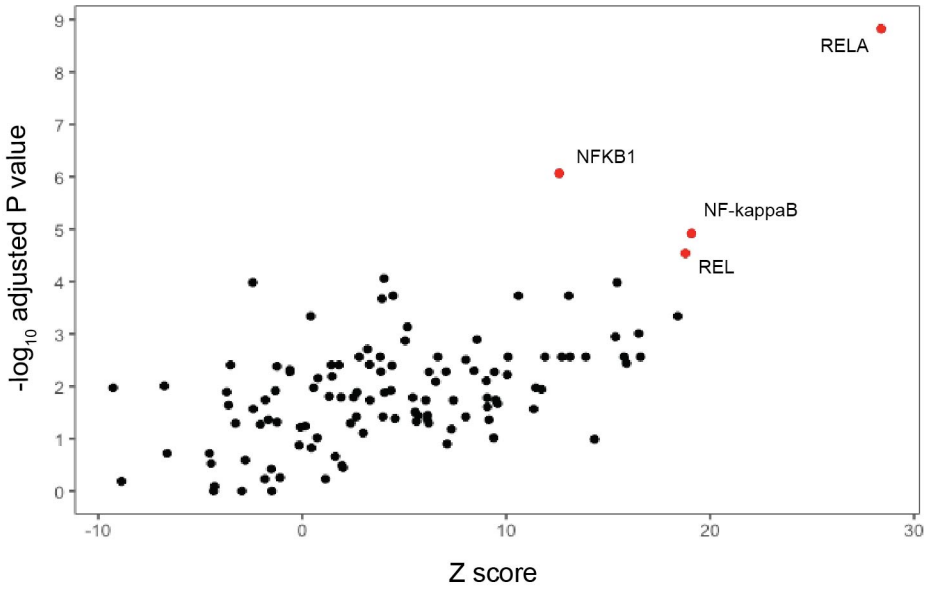


**Supplemental Figure S13.** OPOSSUM Analysis for detection of over-represented conserved transcription factor binding sites at promoters of genes upregulated in stimulated RLTPR (p.Q575E) cells. The plots of show adjusted *P* values as a function of Z scores.

**Supplemental Figure S14. Model by which RLTPR p.Q575E potentiates T cell receptor-dependent NF-κB signaling.**

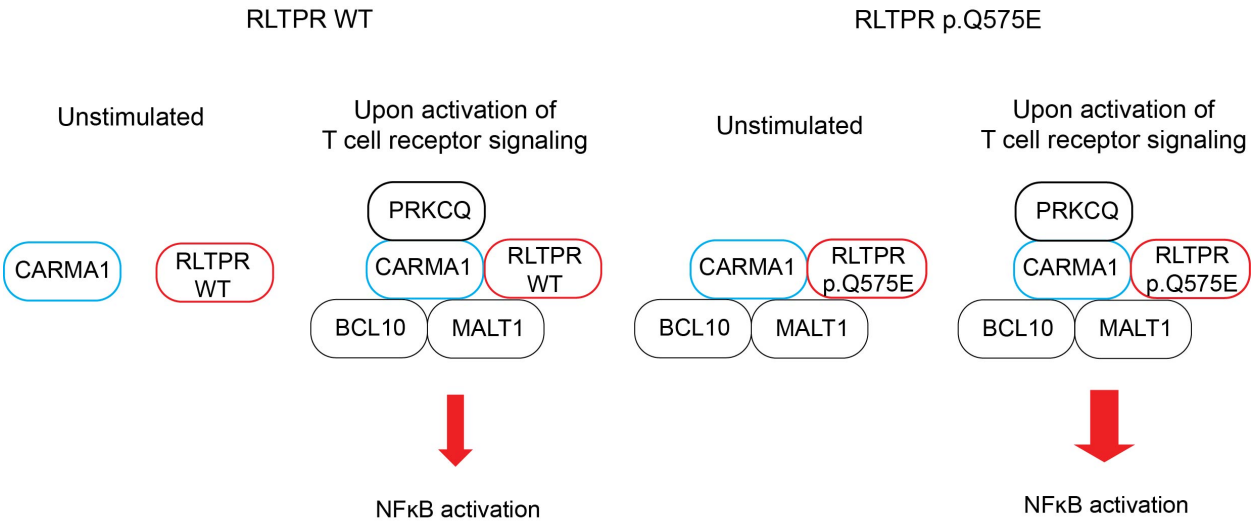


**Supplemental Figure S14.** Model by which RLTPR p.Q575E potentiates T cell receptor-dependent NF-κB signaling. RLTPR acts as scaffolding protein to form signaling complex with CARMA1 and function to transmit the signal in the NF-κB pathway. RLTPR WT can bind with CARMA1 only after stimulation.[25] In contrast, RLTPR p.Q575E forms a complex with CARMA1 even without stimulation. However, the complex is inert in the absence of additional signals downstream of the T cell receptor.

## References


1. Choi J, Goh G, Walradt T, et al. Genomic landscape of cutaneous T cell lymphoma. *Nat Genet*. 2015;47(9):1011-1019.
2. Ungewickell A, Bhaduri A, Rios E, et al. Genomic analysis of mycosis fungoides and Sezary syndrome identifies recurrent alterations in TNFR2. *Nat Genet*. 2015;47(9):1056-1060.
3. McGirt LY, Jia P, Baerenwald DA, et al. Whole-genome sequencing reveals oncogenic mutations in mycosis fungoides. *Blood*. 2015;126(4):508-519.
4. Vaque JP, Gomez-Lopez G, Monsalvez V, et al. PLCG1 mutations in cutaneous T-cell lymphomas. *Blood*. 2014;123(13):2034-2043.
5. Kiel MJ, Sahasrabuddhe AA, Rolland DC, et al. Genomic analyses reveal recurrent mutations in epigenetic modifiers and the JAK-STAT pathway in Sezary syndrome. *Nat Commun*. 2015;6:8470.
6. Wang L, Ni X, Covington KR, et al. Genomic profiling of Sezary syndrome identifies alterations of key T cell signaling and differentiation genes. *Nat Genet*. 2015;47(12):1426-1434.
7. da Silva Almeida AC, Abate F, Khiabanian H, et al. The mutational landscape of cutaneous T cell lymphoma and Sezary syndrome. *Nat Genet*. 2015;47(12):1465-1470.
8. Woollard WJ, Pullabhatla V, Lorenc A, et al. Candidate driver genes involved in genome maintenance and DNA repair in Sezary syndrome. *Blood*. 2016;127(26):3387-3397.
9. Prasad A, Rabionet R, Espinet B, et al. Identification of Gene Mutations and Fusion Genes in Patients with Sezary Syndrome. *J Invest Dermatol*. 2016;136(7):1490-1499.
10. Yoo HY, Sung MK, Lee SH, et al. A recurrent inactivating mutation in RHOA GTPase in angioimmunoblastic T cell lymphoma. *Nat Genet*. 2014;46(4):371-375.
11. Nagata Y, Kontani K, Enami T, et al. Variegated RHOA mutations in adult T-cell leukemia/lymphoma. *Blood*. 2016;127(5):596-604.
12. Vallois D, Dobay MP, Morin RD, et al. Activating mutations in genes related to TCR signaling in angioimmunoblastic and other follicular helper T-cell-derived lymphomas. *Blood*. 2016;128(11):1490-1502.
13. Kataoka K, Nagata Y, Kitanaka A, et al. Integrated molecular analysis of adult T cell leukemia/lymphoma. *Nat Genet*. 2015;47(11):1304-1315.
14. Sakata-Yanagimoto M, Enami T, Yoshida K, et al. Somatic RHOA mutation in angioimmunoblastic T cell lymphoma. *Nat Genet*. 2014;46(2):171-175.
15. Palomero T, Couronne L, Khiabanian H, et al. Recurrent mutations in epigenetic regulators, RHOA and FYN kinase in peripheral T cell lymphomas. *Nat Genet*. 2014;46(2):166-170.
16. Crescenzo R, Abate F, Lasorsa E, et al. Convergent mutations and kinase fusions lead to oncogenic STAT3 activation in anaplastic large cell lymphoma. *Cancer Cell*. 2015;27(4):516-532.
17. Roberti A, Dobay MP, Bisig B, et al. Type II enteropathy-associated T-cell lymphoma features a unique genomic profile with highly recurrent SETD2 alterations. *Nat Commun*. 2016;7:12602.
18. Kandoth C, McLellan MD, Vandin F, et al. Mutational landscape and significance across 12 major cancer types. *Nature*. 2013;502(7471):333-339.

19. Zhao S, Bellone S, Lopez S, et al. Mutational landscape of uterine and ovarian carcinosarcomas implicates histone genes in epithelial-mesenchymal transition. *Proc Natl Acad Sci U S A*. 2016;113(43):12238-12243.
20. Arcila ME, Drilon A, Sylvester BE, et al. MAP2K1 (MEK1) Mutations Define a Distinct Subset of Lung Adenocarcinoma Associated with Smoking. *Clin Cancer Res*. 2015;21(8):1935-1943.
21. Pinzaru AM, Hom RA, Beal A, et al. Telomere Replication Stress Induced by POT1 Inactivation Accelerates Tumorigenesis. *Cell Rep*. 2016;15(10):2170-2184.
22. Vogelstein B, Papadopoulos N, Velculescu VE, Zhou S, Diaz LA, Jr., Kinzler KW. Cancer genome landscapes. *Science*. 2013;339(6127):1546-1558.
23. Wei Y, Zhang Y, Derewenda U, et al. Crystal structure of RhoA-GDP and its functional implications. *Nat Struct Biol*. 1997;4(9):699-703.
24. Wilkinson GW, Akrigg A. Constitutive and enhanced expression from the CMV major IE promoter in a defective adenovirus vector. *Nucleic Acids Res*. 1992;20(9):2233-2239.
25. Roncagalli R, Cucchetti M, Jarmuzynski N, et al. The scaffolding function of the RLTPR protein explains its essential role for CD28 co-stimulation in mouse and human T cells. *J Exp Med*. 2016;213(11):2437-2457.